

# Collective Transport in Random Media: From Superconductors to Earthquakes

Lectures at Summer School on  
 “Fundamental Problems in Statistical Mechanics IX”  
 August 20-23, 1997

Daniel S. Fisher  
 Physics Department, Harvard University  
 Cambridge, MA 02138  
 fisher@cmt.harvard.edu

## Abstract

In these lectures, a variety of non-equilibrium transport phenomena are introduced that all involve, in some way, elastic manifolds being driven through random media. A simple class of models is studied focussing on the behavior near to the critical “depinning” force above which persistent motion occurs in these systems. A simple mean field theory and a “toy” model of “avalanche” processes are analyzed and used to motivate the general scaling picture found in recent renormalization group studies. The general ideas and results are then applied to various systems: sliding charge density waves, critical current behavior of vortices in superconductors, dynamics of cracks, and simple models of a geological fault. The roles of thermal fluctuations, defects, inertia, and elastic wave propagation are all discussed briefly.

## I. Introduction

Many phenomena in nature involve transport of material or some other quantity from one region of space to another. In some cases transport occurs in systems that are close to equilibrium with the transport representing only a small perturbation such as flow or electrical current in a metal, while in other cases it involves systems that are far from equilibrium such as a landslide down a mountain, or a drop of water sliding down an irregular surface. Sometimes, particles or other constituents move relatively independently of

each other like the electrons in a metal, while in other situations the interactions play an important role, as in the landslide and the water droplet.

If the interactions are strong enough, all the particles (or other constituents) move together and the macroscopic dynamics involves only a small number of degrees of freedom. This is the case for a small water drop on, e.g. wax paper, which slides around while retaining its shape. But if the interactions are not so strong relative to the other forces acting on the constituents, then the transport involves in an essential way *many interacting degrees of freedom*. This is the case for a larger water drop on an irregular surface for which the contact line between the droplet and the surface continually deforms and adjusts its shape in response to the *competition* between the surface tension of the water and the interactions with the substrate [36][16]. Such a moving drop and the landslide are examples of non-equilibrium *collective transport phenomena*, which will be the general subject of these lectures.

This is, of course, an impossibly broad subject! We must thus narrow the scope drastically. Although the range of systems discussed here will, nevertheless, be reasonably broad, we will primarily focus on systems in which the interactions are strong enough so that the transported object (or at least some part of it) is *elastic*. We will use this in a general and somewhat loose sense that the transported object has enough integrity that if one part of it moves a long distance then so, eventually, must the other parts as well. Thus the fluid drop is elastic if it does not break up—i.e. its perimeter retains its integrity—while a landslide is not elastic as some rocks will fall much further than others and the relative positions of the rocks will be completely jumbled by the landslide.

We will be interested in systems in which the medium in which the transport occurs has static random heterogeneities (“quenched randomness”) which exert forces on the transported object that depend on where it is in space.

Examples we will discuss are: interfaces between two phases in random media [28][2], such as between two fluids in a porous medium [37], or domain walls in a random ferromagnetic alloy; lattices of vortices in dirty type II superconductors [34]; charge density waves which are spatially periodic modulations of the electron density that occur in certain solids [35][4][3]; and the motion of geological faults [43],[5]. In addition to the contact line of the fluid drop already mentioned [36],[16], another well known—but poorly understood—example that we will, however, not discuss is solid-on-solid fric-

tion.

In all of these systems, a driving force, call it  $F$ , can be applied which acts to try to make the object move, but this will be resisted by the random “pinning” forces exerted by the medium or substrate. The primary questions of interest will involve the response of the system to such an applied driving force [47]. If  $F$  is small, then one might guess that it will not be sufficient to overcome the resistance of the pinning forces; sections of the object would just move a bit and it would deform in response to  $F$ , but would afterwards be at rest. [Note that in most of what follows, we will ignore fluctuations so that the motion is deterministic and the objects can be said to be stationary.] If the force is increased, some segment might go unstable and move only to be stopped by stronger pinning regions or neighboring segments. But for large enough  $F$ , it should be possible to overcome the pinning forces—unless they are so strong that the object is broken up, an issue we will return to at the end—and the object will move, perhaps attaining some steady state velocity  $v$ .

Basic questions one might ask are: is there a *unique*, history independent force,  $F_c$  separating the static from the moving regimes? How does  $v$  depend on  $F$  (and possibly on history)? Are there some kinds of non-equilibrium critical phenomena when  $v$  is small? How does the system respond to an additional time or space dependent applied force? These are all *macroscopic* properties of the system.

But we will also be interested in some *microscopic* properties: how can one characterize (statistically) the deformations of the object when it is stationary [38]? The dynamic deformations and local velocities when it is moving? The response to a small local perturbation? etc.

Motivated by possible analogies with equilibrium phase transitions [33], we can ask if there are *scaling laws* that might obtain near a critical force which relate, for example, the characteristic length scale  $L$ , for some process, to its characteristic time scale,  $\tau$ , via a power law relation of the form:

$$\tau \sim L^z \tag{1}$$

Trying to answer some of these questions—and to pose other more pointed questions—is the main aim of these lectures. In the next few sections a particular system and its natural (theoretical) generalizations will be studied and tools and ideas developed. In the last section, these are tentatively

applied to various physical systems and some of the complicating features left out of the simple model systems are discussed. This leads naturally to many open questions.

## II. Interfaces and Models

In order to develop some of the general ideas—both conceptual and computational—we will focus initially on an *interface* between two phases that is driven by an applied force through an inhomogeneous medium [28],[2]. The essential ingredients of a model of this system are: the forces of sections of the interface on nearby sections, i.e. the elasticity of the interface caused by its interfacial tension; the preference of the interface for some regions of the system over others due to the random heterogeneities; and some dynamical law which governs the time evolution of the local interface position.

We will initially make several simplifying approximations, which we will come back and examine later. First, we assume that the interface is not too distorted away from a flat surface normal to the direction ( $z$ ) of the driving force so that its configuration can be represented by its displacement field  $u(\vec{r})$  away from a flat reference surface. The coordinates  $\vec{R} = (x, y, z)$  of points on the surface are then

$$(x, y) = \vec{r} \text{ and } z = u(\vec{r}). \quad (2)$$

Second, we will assume that the dynamics are purely *dissipative* i.e. that inertia is negligible—a good approximation in many physical situations. Keeping only the lowest order terms in deviations from flat, we then have

$$\eta \frac{\partial u(\vec{r}, t)}{\partial t} = F + \sigma(\vec{r}, t) - f_p[\vec{r}, u(\vec{r}, t)] \quad (3)$$

with  $F$  representing the driving force on the interface,  $f_p(\vec{R})$  representing the random “pinning” forces of the heterogeneous medium on the interface which we assume for the present are not history or velocity dependent;  $\eta$  a dissipative coefficient; and

$$\sigma(\vec{r}, t) = \int d\vec{r}' \int_0^t dt' J(\vec{r} - \vec{r}', t - t') [u(\vec{r}', t') - u(\vec{r}, t)] \quad (4)$$

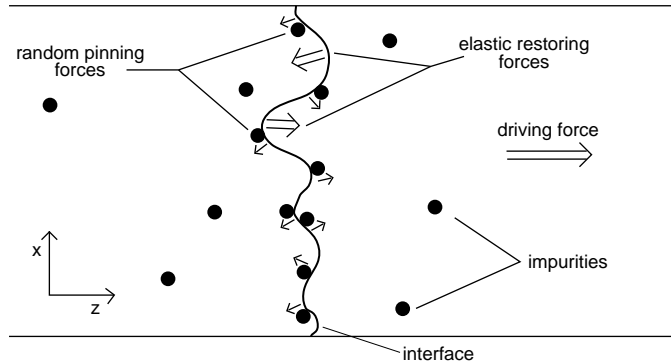


Figure 1: Schematic of a one-dimensional interface in a two dimensional disordered system illustrating the forces acting on the interface.

the “stress” on the interface from its elasticity which is “transmitted” by the kernel  $J(\vec{r}, t)$ . Short range elasticity of the interface corresponds to

$$J\alpha\delta(t)\nabla^2\delta(\vec{r}). \quad (5)$$

A schematic of such an interface and the forces acting on it is shown in Fig 1.

Keeping in mind some of the other problems of interest [36],[6, 30] in addition to interfaces, we will abstract to a more general problem of a  $d$ -dimensional elastic “manifold”— $d = 2$  for the interface—with more general interactions, which can be long-range, embodied in  $J(\vec{r}, t)$ . In addition to the form of  $J(\vec{r}, t)$ , the system will be characterized by the statistics of the pinning forces which impede interface motion near points where the interface has lower (free) energy;  $f_p(\vec{R})$  will generally have only short-range correlations in space, i.e., in both  $u - u'$  and  $\vec{r} - \vec{r}'$ . Even with these simplifying assumptions, the model Eqs (3, 4) is impossible to analyze fully due to the non-linearities implicit in the  $u$  dependence of  $f_p(\vec{r}, u)$ . Nevertheless a lot of the qualitative behavior can be guessed.

If the driving force is sufficiently small, then it will be insufficient to overcome the pinning forces. But if  $F$  is increased slowly, it may overcome the pinning of some small segment of the interface which can then jump forwards only to be stopped by stronger pinning forces or by the elastic forces from neighboring still-pinned parts of the interface. But if the drive

is larger, the neighboring regions may themselves not be strongly enough pinned to resist the increase in stress from the jumping section and may themselves jump forward leading to an “avalanche” of some larger region of the interface; this process might or might not eventually stop [38]. If the force is large enough—and certainly if it exceeds the maximum  $f_p$ —then it is not possible for the interface to be pinned and the interface will move forward with some average velocity  $\bar{v}$ , albeit via very jerky motion both in space and time.

In addition to the basic questions raised in the Introduction, we will be interested, in the regime where avalanches can stop, in the statistical properties of the sizes and dynamics of the avalanches [38][9][2].

The existence of a *unique critical force* can be established by a simple convexity argument that is valid if  $J(\vec{r}, t)$  is non-negative [26]. If two configurations  $u_a$  and  $u_b$  of the interface at time  $t_0$  have the property that one is “ahead” of the other, i.e.  $u_a(\vec{r}, t_0) > u_b(\vec{r}, t_0)$  for all  $\vec{r}$ ; then  $u_a$  will be ahead of  $u_b$  at all later times. This can be seen by assuming the contrary and then considering the putative first time  $t_1 > t_0$  at which there is a point of contact; say  $u_a(\vec{r}_1, t_1) = u_b(\vec{r}_1, t_1)$  at some  $\vec{r}_1$ . Then

$$\begin{aligned} & \frac{\partial}{\partial t} [u_a(\vec{r}_1, t) - u_b(\vec{r}_1, t)] |_{t=t_1} = \sigma[\vec{r}_1, \{u_a\}] - \sigma[\vec{r}_1, \{u_b\}] \\ & = \int d\vec{r}' \int^{t_1} dt' J(\vec{r}_1 - \vec{r}', t_1 - t') [u_a(\vec{r}', t') - u_b(\vec{r}', t')] > 0 \end{aligned} \quad (6)$$

since the pinning force at  $\vec{r}_1$  is the same in both configurations and therefore cancels out. By assumption the last expression in Eq (6) is positive as long as  $J$  is non-negative so that for  $t > t_1$ ,  $u_a$  is again ahead of  $u_b$  violating the assumption.

The condition that

$$J(\vec{r}, t) \geq 0 \quad (7)$$

for all  $\vec{r}, t$  plays an important role in the theoretical analysis and frequently also in the physics of these types of systems. We will refer to models with this convexity property as *monotonic*; they have the property that if the displacements and the driving force  $F(t)$  increase monotonically with time, then so will the total “pulling force”—see later—on any segment. Except in the final section we will *focus solely on monotonic models*.

We have shown that in monotonic models one configuration that is initially behind cannot “pass” another that is ahead of it [26]; therefore station-

ary and continually moving solutions *cannot coexist* at the same  $F$ ; therefore  $F_c$  is *unique*. This is a big simplification and one that will not occur generally, in particular not in some of the systems that we discuss in the last section.

For forces well above  $F_c$ , one can use perturbative methods to study the effects of the random pinning and compute, for example: the mean velocity,  $\bar{v}(F)$ , the spatio-temporal correlations of the local velocities, and responses to additional applied forces [4]. Near  $F_c$ , however, life is much more complicated as is usually the case near critical points—but for conventional equilibrium critical points the theoretical framework for dealing with the complexities is well established [33]. The most interesting behavior occurs in the critical regime; in particular one might expect processes—such as avalanches—to occur on a wide range of length and time scales. In order to make real progress, we will have to—at least initially—make further simplifications or approximations.

One of the lessons from equilibrium critical phenomena is that analyzing simple models exactly or by controlled approximations is more useful than analyzing more realistic models by uncontrolled approximations; we will thus take the former route. But we must first find some clues as to what simplifications preserve—what we hope will be—the most essential features.

Near the critical force, at any given time most of the interface will be moving very slowly if at all so that the left hand side of Eq (3) will be close to zero. Thus a first try might be to replace the actual dynamics with the *adiabatic* approximation that the forces at every point always balance exactly. Let us focus on one point  $\vec{r}$  on the interface and divide the stress  $\sigma(\vec{r})$ , Eq (4), into the local part  $\tilde{J}u(\vec{r}, t)$  and the non-local part,  $f_\sigma$ , involving  $u(\vec{r}', t')$  for  $r' \neq r$  with

$$\tilde{J} \equiv \int d\vec{r}' \int dt' J(\vec{r}', t'). \quad (8)$$

We then have a balance between the local force,  $f_p + \tilde{J}u$  and the *pulling force*,

$$\phi(\vec{r}, t) \equiv f_\sigma(\vec{r}, t) + F. \quad (9)$$

The adiabatic approximation corresponds to

$$f_p(\vec{r}, t) \approx \phi(\vec{r}, t) - \tilde{J}u(\vec{r}, t). \quad (10)$$

But generally, because of the non-linearities in  $f_p(u)$ , for a fixed  $\phi$  “applied”

to  $u(\vec{r})$  there can be multiple values of  $u$  which satisfy Eq (10); as we shall see these play an important role in the physics.

At this point, it is helpful to be more concrete. Let us consider a simple model of the pinning consisting of pinning sites  $u_\alpha^p(\vec{r})$  distributed for fixed  $\vec{r}$  with random spacings between the  $u_\alpha^p(\vec{r})$ ,

$$\Upsilon_\alpha(\vec{r}) \equiv u_{\alpha+1}^p(\vec{r}) - u_\alpha^p(\vec{r}) \quad (11)$$

drawn, for each  $\vec{r}$ , independently from a distribution  $\Pi(\Upsilon)d\Upsilon$ . The pinning force  $f_p[(\vec{r}, u(\vec{r}))] = 0$  except if  $u(\vec{r})$  is equal to one of the pinning positions, while for  $u(\vec{r}) = u_\alpha^p(\vec{r})$ ,  $f_p$  can take any value between zero and a *yield strength*,  $f_y$ , which is the same for each pin. A typical realization of the pinning force  $f_p(u)$  on some segment of the interface is plotted in Fig. 2a. Note that for a *fixed*  $\phi$ , there are *several possible values of*  $u$  given by the intersection of the line  $\phi - \tilde{J}u$  with  $f_p(u)$ .

If  $\phi$  is increased, then the particular (history dependent) force-balanced position  $u(\phi)$  that the interface point is following adiabatically can become unstable—for example, the configuration denoted by the circle in Fig. 2a—and  $u$  must jump to a new position. During the jump  $\eta \frac{\partial u}{\partial t}$  is clearly *not* small and Eq (10) will not be satisfied. But if such jumps occur more rapidly than the time scales of interest then their primary effect will be a time lag between the actual  $u[\phi(t)]$  and an adiabatic solution  $u_{ad}[\phi(t)]$  to Eq (3). A way to capture this feature while preserving both the physics of the time delays and the conceptually simplifying separation of motion into adiabatic and jump parts (with  $\frac{\partial u}{\partial t} = 0$  in the adiabatic parts for the pinning model illustrated in Fig 2), is to require

$$u[\phi(\vec{r}, t)] = u_{ad}[\phi(\vec{r}, t - t_d)] \quad (12)$$

with some fixed (microscopic) delay time  $t_d$ . This is illustrated in Fig 2a. Note that, formally, this can be accomplished, by taking  $\eta \rightarrow 0$  and  $J(\vec{r}, t) = J(\vec{r})\delta(t - t_d)$ .

### III. Infinite-range model: mean field theory

The above discussion in terms of the local pulling force  $\phi(\vec{r}, t)$  suggests that we could try to analyze the system crudely by assuming that the spatial and temporal fluctuations in  $\phi(\vec{r}, t)$  are small so that  $\phi$  can be replaced by



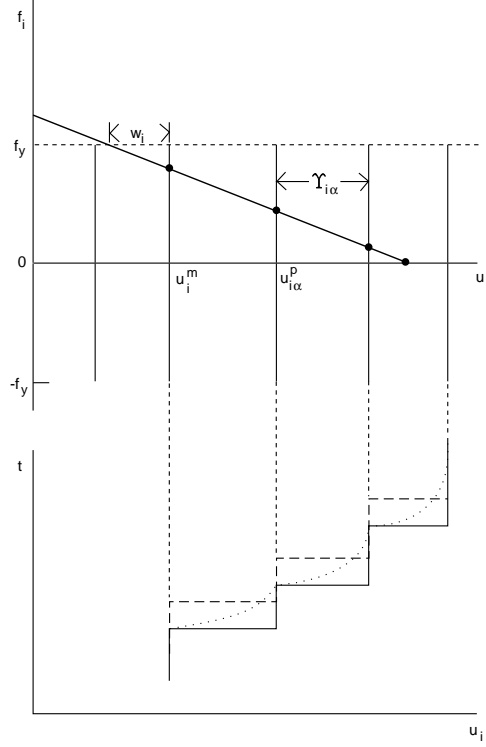


Figure 2: a) Simple model of the forces on one segment of an interface. The segment can be pinned at the positions,  $u_{i\alpha}^p$ , of the vertical lines at which the pinning force can take any value up to the yield strength  $f_y$ . The intersections of the “comb” representing the pinning force  $f_p(u_i)$  and the diagonal line  $\varphi - \tilde{J}u_i$  with  $\varphi$  the total pulling force from the applied force and other segments of the interface, are the possible stationary positions of  $u_i$  indicated by the dots. The one of these with the smallest  $u_i$ ,  $u_i^m$ , plays a special role as discussed in the text. The amount  $\Delta\varphi$  that  $\phi$  needs to increase by to depin the segment from this pinning position is  $w_i\tilde{J}$ . b) Dynamics of the same segment of the interface as the pulling force is increased. The actual  $u_i(t)$  (dotted), the adiabatic approximation to this (solid), and the time delayed approximation (dashed) that is used in the analysis in the text are all shown.

some sort of time dependent average  $\overline{\phi}(t)$  which would then need to be determined self-consistently from the behavior of the neighboring regions that contribute to the stress at our chosen point  $\vec{r}$  [4]. This is very analogous to the well known *mean field* approximation to conventional phase transitions: for example, in a magnetic system the statistical mechanics (or dynamics) of a single spin  $S(\vec{r})$  in the presence of a local effective field,  $h_{eff}(\vec{r})$  from its neighbors—the mean field—is analyzed and the mean field determined self-consistently from the condition that at all points the *assumed*  $\langle S \rangle$  entering the mean field  $h_{eff}(\vec{r}) = \sum_{\vec{r}'} J(\vec{r} - \vec{r}') \langle S(\vec{r}') \rangle$ , is the same as the *computed*  $\langle S \rangle$ . One of the advantages of this approximation is that it has a well-defined regime of validity: in the limit that the range of the interaction is very long [or more properly that the effective number of neighbors,  $(\sum_{\vec{r}'} |J(\vec{r}')|)^2 / \sum_{\vec{r}'} |J(\vec{r}')|^2$  is large] then the mean field theory becomes exact. But—users beware!—for fixed, but finite range interactions it can still fail near critical points as we shall see.

In order to obtain analytic results in at least *some* model, we will study a strictly mean field limit where each discrete segment of the interface—we label simply by a subscript  $i$  since it is no longer really a spatial coordinate—has an independent random pinning force  $f_p^i(u_i)$ , of the form in Fig 2, and the  $N$  segments are *all* coupled together by a uniform coupling

$$J_{ij} = \frac{J(t)}{N} \quad (13)$$

i.e., *infinite range* forces. (Note that Eq (13) includes a self-coupling piece but its effects are negligible in the desired  $N \rightarrow \infty$  limit.) Much can be done for general non-negative  $J(t)$  and more complicated forms of  $f_p(u)$  using the actual dynamical evolution Eq (3) [3], but to keep things simple we will use the time-delayed adiabatic approximation discussed above with

$$J(t) = \tilde{J}\delta(t - t_d); \quad (14)$$

and the form of  $f_p^i$  of Fig 2a with independent randomness for each  $i$ . For simplicity, we will focus on the strong pinning limit which corresponds to

$$f_y > \tilde{J}\Upsilon_{max}. \quad (15)$$

It is left to the reader to show that including some of the more “realistic” features within the infinite range model does not change the qualitative or other universal aspects of the results.

Our task is now simple, at least in principle: we assume some mean field

$$\bar{\phi}(t) = F + \tilde{J} \frac{1}{N} \sum_i u_i(t - t_d), \quad (16)$$

compute the evolution of each  $u_i(t)$  (from  $\phi_i = \bar{\phi}$  for all  $i$ ) from some set of initial conditions, and then adjust our guessed  $\bar{\phi}(t)$  until the computed

$$\langle u(t) \rangle \equiv \frac{1}{N} \sum_i u_i(t) \quad (17)$$

is equal to  $[\bar{\phi}(t + t_d) - F] / \tilde{J}$  for all  $t$ .

We first try the simplest possibility: a *constant*  $\bar{\phi}(t)$ . We can proceed graphically. From Fig 2a we select for each  $i$  one of the possible stationary values of  $u_i$ . We have many choices; the only constraint being that

$$\langle u \rangle = (\bar{\phi} - F) / \tilde{J}. \quad (18)$$

But we must be careful: If we start choosing too many large  $u_i$ 's, we may find that  $\langle u \rangle$  will become too large. We can thus ask: what are the minimum and maximum possible  $\langle u \rangle$  for a given  $\bar{\phi}$ ? The minimum will turn out to be of primary interest so we focus on this: for each  $i$ , the minimum  $u_i$ ,  $u_i^m(\bar{\phi})$  corresponds to the first pinning position—i.e. one of the  $\{u_{i\alpha}^p\}$ —to the right of the intersection of the line  $f = \phi - \tilde{J}u$  with the line  $f = f_y$  that passes through the tips of the “comb”—representing the yield strength—in Fig. 2a<sup>1</sup>. Since the peaks are randomly positioned,

$$\langle u_i \rangle^{min} = \langle u_i^m(\bar{\phi}) \rangle = (\bar{\phi} - f_y) / \tilde{J} + \langle w_i \rangle \quad (19)$$

with  $w_i$  the distance to the next pin which has the distribution<sup>2</sup>:

$$\text{Prob}(w) = \int_w^\infty \frac{1}{\Upsilon} \left[ \frac{\Upsilon \Pi(\Upsilon) d\Upsilon}{\overline{\Upsilon}} \right]. \quad (20)$$

---

<sup>1</sup>The strong pinning condition  $f_y > \tilde{J}\Upsilon_{max}$  ensures that  $u_i^m$  is at a pinning position. The general case can be worked out similarly

<sup>2</sup>We use notations like “Prob( $w$ )” to mean the probability that the continuous variable  $w$  is in the range  $w$  to  $w+dw$ , divided by  $dw$ ; i.e. Prob( $w$ ) is the probability *density* (usually called by physicists “distribution”) of  $w$ . One must remember, however, that if variables are changed e.g. from  $w$  to  $w'$ , then there is a Jacobian needed: Prob( $w'$ ) =  $(\frac{dw}{dw'})$  Prob( $w$ ).

Here the quantity in parentheses is the probability distribution that a random point is in an interval of width  $\Upsilon$  between pins; this includes the factor of  $\Upsilon/\overline{\Upsilon}$  with

$$\overline{\Upsilon} \equiv \int_0^\infty \Upsilon \Pi(\Upsilon) d\Upsilon \quad (21)$$

because of the presence of more points in wider intervals. Integration of Eq (20) by parts yields  $\langle w \rangle = \overline{\Upsilon^2}/(2\overline{\Upsilon})$  so that

$$\langle u_i \rangle^{min} = (\overline{\phi} - f_y)/\tilde{J} + \frac{\overline{\Upsilon^2}}{2\overline{\Upsilon}} = \frac{F}{\tilde{J}} + \langle u_i \rangle - \frac{f_y}{\tilde{J}} + \frac{\overline{\Upsilon^2}}{2\overline{\Upsilon}} \quad (22)$$

from Eqs (16) and (19). For self consistency, we must therefore have

$$F \leq F_c = f_y - \tilde{J} \frac{\overline{\Upsilon^2}}{2\overline{\Upsilon}} \quad (23)$$

a non-trivial result for the *critical force* above which no static solutions are possible. Note that as the interaction strength,  $\tilde{J}$ , is increased, the critical force *decreases*. Physically, this is a consequence of the elasticity causing the system to average over the randomness more effectively: pulling a stiff object over a rough surface is easier than pulling a flexible one.

For  $F < F_c$  the number of stable solutions,  $N_s$  will be exponentially large with an “entropy” per segment  $\frac{\ln N_s}{N}$  which is of order one well below  $F_c$  but decreases to zero at  $F_c$  as most of the  $u_i$ ’s will then need to take their minimum values to ensure self-consistency.

What happens as  $F$  is increased slowly from below  $F_c$  so that the non-adiabaticity is negligible? Since this will certainly result in  $\langle u \rangle$  and hence  $\overline{\phi}$  increasing, we can understand the behavior from Fig 2. As  $\overline{\phi}$  increases, some segments become unstable and jump to their next pinning positions. But this cannot happen unless they are stuck on the pin with smallest  $u_{i\alpha}^p$ , i.e.  $u_i^m(\overline{\phi})$ . Furthermore, after a jump  $u$  will again be on the new smallest  $u_{i\alpha}^p$  for the increased  $\overline{\phi}$ . Thus the  $u_i$ ’s are gradually swept to their minimum stable positions as  $F$  is increased towards  $F_c$ .

Above  $F_c$ , the segments continue to jump from one  $u_i^m(\overline{\phi})$  to the next. But now the time delays must play a role. If we assume a solution which progresses uniformly on average,  $\langle u \rangle = vt$ , then

$$\overline{\phi} = \tilde{J}vt - \tilde{J}vt_d + F. \quad (24)$$

[Note that to ensure that  $u$  does not stop between pins, we again need the strong pinning condition  $\tilde{J}\Upsilon_{max} < f_y$ ] With all  $u_i = u_i^m(\bar{\phi})$ , our earlier analysis immediately yields self-consistency only when

$$\bar{v} = \frac{F - F_c}{\tilde{J}t_d} \quad (25)$$

so that near criticality

$$\bar{v} \sim (F - F_c)^\beta \quad (26)$$

with the *critical exponent*

$$\beta = \beta_{MF} = 1 \quad (27)$$

in this infinite range mean-field model [41].

Note that a comparison of Eq (25) for  $F \gg F_c$  and the original dynamic equation (3), suggests that a natural choice is  $t_d = \frac{\eta}{J}$  so that  $\bar{v} = \frac{F}{\eta}$  for large  $F$ . The actual non-adiabatic processes can be seen to give rise to an effective  $t_d$  of roughly this magnitude. But the breakdown of the jump approximation for large  $F$  will make  $\bar{v}$  *not* strictly linear for  $F > F_c$ . Nevertheless near  $F_c$ , the mean velocity will still be characterized by the exponent  $\beta = 1$ . A typical mean-field  $\bar{v}(F)$  curve is shown in Fig 3.

In addition to the critical force and the steady state velocity, in our simple mean field model one can compute other “macroscopic” properties e.g., hysteresis loops as  $F$  is increased and decreased—sketched in Fig 4 [9]—and responses to a time dependent additional driving force which in the pinned phase will depend, due to the metastability, on the past history, the sign of the perturbations, etc [4]. Some of the properties—like the exponent  $\beta$ —will be universal within a broad class of mean field models, while others will depend on details. Nevertheless, substantial qualitative insight can be obtained that gives useful clues to the behavior of finite—in particular real two-dimensional—interfaces. Furthermore, experience with equilibrium critical phenomena suggests that some of the asymptotic *forms* near  $F_c$ , such as Eq (25) will be correct in realistic models if the dimension of the “interface” is sufficiently large or the interactions are sufficiently long range [48][16]. We will return to these questions later, but for now we stick to the simple mean field model and ask what can be learned about “microscopic” properties, in particular the properties of avalanches that occur as the driving force is increased towards  $F_c$ .

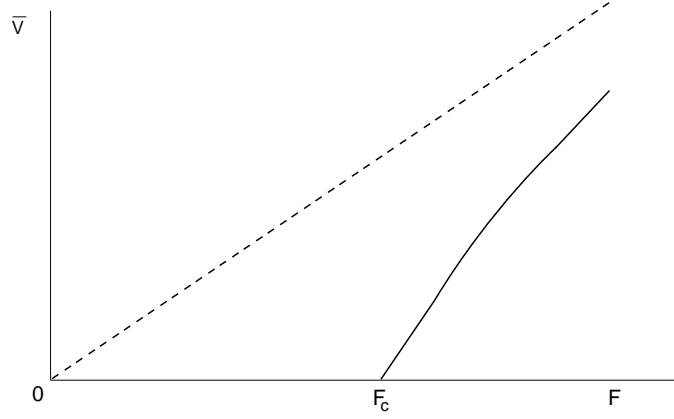


Figure 3: Velocity versus driving force in a typical mean field model is indicated by the solid line. Note the linear dependence of  $v$  on  $F$  just above  $F_c$ . The dashed line is the behavior in the absence of pinning.

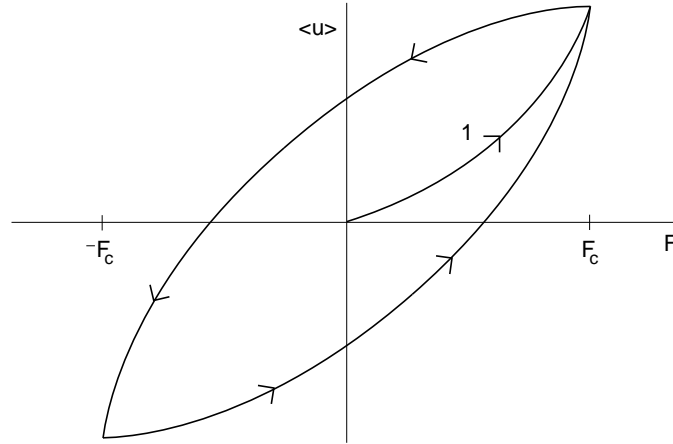


Figure 4: Schematic of hysteresis loops that occur as the force is increased from zero to the critical force, decreased to the critical force in the opposite direction, and then cycled between these values. The direction of change of  $F$  is indicated by the arrows with the “1” denoting the first increase.

## IV. Avalanche statistics and dynamics

In the mean field model introduced in the previous section, the statistics and other properties of the avalanches of jumps that occur as the driving force is increased slowly can be worked out in substantial detail [39][44]. We will carry out the analysis using methods which can be generalized to provide useful information about the behavior with more realistic interactions.

Let us consider what happens for  $F < F_c$  when  $F$  is increased by a very small amount. If the increase is sufficiently small, then no segments will jump. But a slightly bigger increase—typically of order  $\frac{1}{N}$ —will result in one jump. Let us call the time of this jump  $t = 0$  and measure times in units of the delay time  $t_d$  so that with  $F$  held fixed after the avalanche starts, we have simple discrete time dynamics. The first jump can trigger  $n_1$  other jumps at time  $t = 1$ , with these triggering  $n_2$  further ones at  $t = 2$  etc. As long as the total number of jumps is finite, then in a large system the mean  $\langle u \rangle$ , and hence  $\bar{\phi}$  will have only advanced by an amount of order  $\frac{1}{N}$ . Thus all that will matter is the distribution of segments which are very close to jumping, i.e. those which will jump when  $\bar{\phi}$  is increased by a small amount  $\Delta\varphi_i$ . From Fig. 2a, we see that  $\Delta\varphi_i = \tilde{J}w_i$ . For large  $N$ , all but very special ways of preparing the conditions before the avalanche starts will yield a distribution of these small  $\Delta\varphi_i$  which are independent and randomly distributed with (initial-condition dependent) density

$$\rho \equiv \rho(\Delta\varphi_i = 0); \quad (28)$$

$\rho$  thus measures a *local susceptibility to jumping*. We can now immediately conclude something about the mean number of jumps  $\langle n_t \rangle$  at a time  $t$  after the initial jump. Since the  $n_{t-1}$  jumps at time  $t - 1$  will cause an increase in  $\bar{\phi}$  by, on average,  $\tilde{J} \langle \Upsilon \rangle n_{t-1}$  (where we have used  $\langle \Upsilon \rangle$  rather than  $\bar{\Upsilon}$  since the distribution of  $\Upsilon$ 's for the almost unstable segments and hence  $\langle \Upsilon \rangle$  could depend on the initial conditions). This will cause, on average,  $\rho \langle \Upsilon \rangle n_{t-1}$  jumps at time  $t$ , i.e.

$$\langle n_t \rangle = \rho \langle \Upsilon \rangle \tilde{J} \langle n_{t-1} \rangle. \quad (29)$$

The crucial parameter is thus  $\rho \langle \Upsilon \rangle \tilde{J}$ ; if this is greater than one the avalanche will runaway. If the system is below  $F_c$  as we have assumed, it will eventually be stopped only when a finite fraction of the segments have

jumped and the system has found a stable—and more typical—configuration. But if  $\rho < \Upsilon > \tilde{J} < 1$ , then the expected total size of an avalanche

$$s \equiv \sum_i \Delta u_i \quad (30)$$

is simply

$$\langle s \rangle = \frac{\langle \Upsilon \rangle}{1 - \rho \langle \Upsilon \rangle \tilde{J}}. \quad (31)$$

As we shall see however, this is *not* the typical size: even very close to criticality; i.e.

$$\epsilon \equiv 1 - \rho \langle \Upsilon \rangle \tilde{J} \ll 1, \quad (32)$$

most avalanches will be small.

The distribution of avalanche sizes, as well as other interesting information on their dynamics etc., can be obtained from generating function methods. Since these are a widely applicable tool, we will go through some of the details. For simplicity we work in units with

$$\langle \Upsilon \rangle = 1 \quad (33)$$

and

$$\tilde{J} = 1. \quad (34)$$

We are interested in the time evolution of the displacements, in particular the increments

$$\begin{aligned} m_t &= \sum_i [u_i(t) - u_i(t-1)] \\ &= \sum_{\alpha=1}^{n_t} \Upsilon_{t\alpha} \end{aligned} \quad (35)$$

where the  $\{\Upsilon_{t\alpha}\}$  are the magnitudes of the  $n_t$  jumps that occur at time  $t$  (with  $m_t = 0$  if  $n_t = 0$ ). The total size is simply

$$s = \sum_{t=0}^{\infty} m_t. \quad (36)$$

The joint probability distribution of all the  $\{m_t\}$  given the initial jump  $n_0 = 1$

$$P\{m_t\} \equiv \text{Prob}[m_0, m_1, m_2 \dots | n_0 = 1], \quad (37)$$



contains the information of interest. Note that vertical bars as in Eq (37) denote “given”; i.e. conditional probability. It is useful to define a *generating function* of the distribution including all times up to  $T$

$$\Gamma_T\{\mu_t\} \equiv \langle \exp(i \sum_{t=0}^T \mu_t m_t) \rangle_P ; \quad (38)$$

(usually we will drop the  $P$ ). Note that  $\Gamma_T$  is simply the Fourier transform of  $P$  restricted to times  $\leq T$ . We can derive a recursion relation for  $\Gamma_T$  in terms of  $\Gamma_{T-1}$ . For a given  $m_{T-1}$ , the number of jumps triggered at time  $T$  will be Poisson distributed with mean  $\rho m_{T-1}$  i.e.

$$\text{Prob}(n_T | m_{T-1}) = \frac{e^{-\rho m_{T-1}}}{n_T!} (\rho m_{T-1})^{n_T}. \quad (39)$$

Then, since  $m_T$  depends only on  $m_{T-1}$ , we can compute

$$\begin{aligned} & \langle e^{i\mu_T m_T} | \{m_t\}_{t < T} \rangle = \langle e^{i\mu_T m_T} | m_{T-1} \rangle \\ &= \sum_{n_T=0}^{\infty} \left\{ \text{Prob}(n_T | m_{T-1}) \prod_{\alpha=1}^{n_T} \left[ \int d\Upsilon_{T\alpha} \Pi(\Upsilon_{T\alpha}) e^{i\mu_T \Upsilon_{T\alpha}} \right] \right\} \\ &= \exp \left[ \rho m_{T-1} (\langle e^{i\mu_T \Upsilon} \rangle - 1) \right] \end{aligned} \quad (40)$$

The last equality follows from Eq. (39); the resulting expression has similar  $m_{T-1}$  dependence to the  $e^{i\mu_{T-1} m_{T-1}}$  factor in  $\Gamma_{T-1}$ .

We thus find that

$$\Gamma_T[\mu_0, \dots, \mu_T] = \Gamma_{T-1}[\mu_0, \dots, \mu_{T-2}, \lambda_{T-1}] \quad (41)$$

with

$$\lambda_{T-1} = \mu_{T-1} - i\rho(\langle e^{i\lambda_T \Upsilon} \rangle - 1) \quad (42)$$

where

$$\lambda_T = \mu_T. \quad (43)$$

We can now iterate with the recursion relation Eq (42) from the “initial” condition Eq (43), eventually obtaining

$$\Gamma_T\{\mu_t\} = \Gamma_0(\lambda_0\{\mu_t\}) = \langle e^{i\lambda_0\{\mu_t\}\Upsilon} \rangle \quad (44)$$

(since  $n_0 = 1$ ). All the information has thus gone into  $\lambda_0$ . As long as the system is stable, i.e.  $\rho \leq 1$ , we can simply take  $T \rightarrow \infty$  to recover the full information. [If  $\rho > 1$ , then there is a non-zero (and computable) possibility that  $s = \infty$ , and more care is needed.]

To get the probability distribution of  $s$ , we simply set all  $\mu_t = \mu$  and then

$$\text{Prob}(s) = \int_{\mu} e^{-i\mu s} e^{i\lambda^*(\mu)} \quad (45)$$

with

$$\int_{\mu} \equiv \frac{1}{2\pi} \int_{-\infty}^{\infty} d\mu \quad (46)$$

and  $\lambda^*(\mu)$  the (stable) *fixed point* solution to Eq (42). Let us first consider the behavior for large  $s$ . This will be dominated by the singularity in the lower half complex  $\mu$  plane nearest to the real axis—a general property of Fourier transforms that can be seen by deforming the integration contour away from the real axis until it encounters a singularity. We only expect to have large avalanches for

$$\epsilon \equiv 1 - \rho \quad (47)$$

small, so the interesting regime is  $\mu$  and  $\epsilon$  small which suggests  $\lambda^*$  small. We find that to leading order,

$$\lambda^* \approx \frac{[-i\epsilon + \sqrt{-\epsilon^2 + 2ib\mu}]}{b} \quad (48)$$

with

$$b \equiv < \Upsilon^2 > \quad (49)$$

and the sign of the square root that has positive imaginary part for  $\mu$  real chosen. For  $\mu \rightarrow 0$ , this gives  $\lambda^* = 0$  as it must for normalization of probability  $\Gamma\{\mu_t = 0\} = 1$ . The integration contour in Eq (45) can be deformed so that it is dominated by the cut at  $\mu = -\frac{1}{2}i\epsilon^2/b$  for large  $s$  and we thus have, after replacing the dummy variable  $\mu$  by  $\mu - \frac{1}{2}i\epsilon^2/b$  and expanding in small  $\mu$ ,

$$\text{Prob}(s) \approx \int_{\mu} i\sqrt{2i\mu/b} e^{-i\mu s} e^{-s\epsilon^2/(2b)} \quad (50)$$

By “power counting”, we see that the branch cut must yield a  $\frac{1}{s^{\frac{3}{2}}}$  dependence; hence for large  $s$ ,

$$\text{Prob}(s) \sim \frac{e^{-s\epsilon^2/(2b)}}{s^{\frac{3}{2}}} \quad (51)$$

[39]. Note that for small  $\epsilon$ , the mean  $\langle s \rangle$  is dominated by large  $s$  avalanches which are rare since

$$\text{Prob}(s \sim \frac{1}{\epsilon^2}) \sim \text{Prob}(s > \frac{1}{\epsilon^2}) \sim \epsilon. \quad (52)$$

We see from Eq (51) that these yield  $\langle s \rangle \sim \frac{1}{\epsilon}$  as expected.

Two questions now arise: First, can we trust this heuristic calculation? And, second, is the large  $s$ , small  $\epsilon$  behavior in Eq (51) generic? The latter we have answered already: the large  $s$  behavior is the same, (except for the coefficient  $b$ ) as long as  $b = \langle \Upsilon^2 \rangle < \infty$ . [The reader is encouraged to find the behavior associated with a power law tail in the distribution of  $\Upsilon^\dagger$ .

As far as justifying the result Eq (51), for the case in which all the jumps are the same,  $\Upsilon = 1$ , one can compute  $\text{Prob}(s)$  exactly by changing the variable of integration to  $z = e^{i\lambda^*(\mu)}$  so that the integral in Eq (45) circles an  $s$ th order pole at  $z = 0$ . Cauchy's theorem then yields

$$\text{Prob}(s) = e^{-\rho s} \frac{(\rho s)^{s-1}}{s!}, \quad (53)$$

with, of course,  $P(s = 0) = 0$ . From the limiting large  $s$  form

$$s! \approx s^s e^{-s} \sqrt{2\pi s} \quad (54)$$

the asymptotic behavior Eq (51) is found confirming the validity of the approximations made in our first derivation of this result. Note that the  $\rho$  dependence is simply via the  $\frac{1}{\rho}(\rho e^{-\rho})^s$  factor in Eq (53). It is nice that the exact result can be found in this case, but in general, asymptotic methods like those we have used above give more understanding and are more widely applicable. Nevertheless, to convince skeptical colleagues, a few exact results are useful!

In addition to the distribution of avalanche sizes, we are also interested in their temporal evolution. For example, one might ask what is  $\langle m_t | s \rangle$ , i.e. what is the time development of an average event of size  $s$ ? This can be computed using the generating function. If we choose

$$\mu_\tau = \mu \text{ for } \tau \neq t \quad (55)$$

---

<sup>†</sup>Note that arbitrarily large jumps can only occur in models that also have arbitrarily large local yield stresses,  $f_y$ .

and

$$\mu_t = \mu + \nu_t, \quad (56)$$

then

$$\frac{1}{i} \frac{\partial \Gamma_\infty}{\partial \nu_t} \Big|_{\nu_t=0} = \langle n_t e^{i\mu s} \rangle = \frac{\partial \lambda_0}{\partial \nu_t} \Big|_{\nu_t=0} \langle e^{i\lambda^*(\mu)\Upsilon} \rangle \quad (57)$$

whose Fourier transform in  $\mu$  yields

$$\int m_t \text{Prob}(m_t, s) dm_t = \int m_t \text{Prob}(m_t | s) dm_t \text{Prob}(s) = \langle m_t | s \rangle \text{Prob}(s). \quad (58)$$

But by multiple use of the chain rule and Eq (42),

$$\frac{\partial \lambda_0}{\partial \nu_t} = \left( \frac{\partial \lambda_t}{\partial \mu_t} \right)_{\lambda_{t+1}} \left( \frac{\partial \lambda_{t-1}}{\partial \lambda_t} \right)_{\mu_{t-1}} \times \dots \times \left( \frac{\partial \lambda_0}{\partial \lambda_1} \right)_{\mu_0} \quad (59)$$

evaluated with all  $\lambda_\tau = \lambda^*(\mu)$  and all  $\mu_\tau = \mu$ .

For the constant  $\Upsilon = 1$  case we obtain,

$$\frac{\partial \lambda_0}{\partial \nu_t} \Big|_{\nu_t=0} = [\rho e^{i\lambda^*(\mu)}]^t \quad (60)$$

After shifting  $\mu$  as in Eq (50) we see that, for  $\epsilon$  small and  $s$  and  $t$  large,

$$\langle m_t | s \rangle \sim \frac{1}{\text{Prob}(s)} \int_\mu e^{-s\epsilon^2/2} e^{-i\mu s + it\sqrt{2i\mu}}. \quad (61)$$

This will be dominated by  $\mu \sim \frac{1}{s}$  and hence the typical duration of an avalanche  $s$  will be

$$\tau \sim \sqrt{s}. \quad (62)$$

Note that this is much less than the maximum possible duration  $\tau_{max} = s - 1$ . The integral in Eq (61) can be done exactly (by writing  $\mu = -i\frac{x^2}{2}$ ) yielding

$$\langle m_t | s \rangle \approx t e^{\frac{-t^2}{2s}} \quad (63)$$

for large  $s$  independent of  $\rho$ . Again, the behavior for large  $s$  and  $1 \ll t \ll s$  is generic up to a coefficient  $b$  that should appear as in Eq. (51). For the

particular constant  $\Upsilon$  case, the exact result can be computed from Eq (58) yielding

$$\langle m_t | s \rangle = \frac{t+1}{(s-t-1)!} (s-1)! s^{-t} \quad \text{for } 0 \leq t \leq s-1. \quad (64)$$

Note that this result includes the rare tail of events which have total duration  $t$  of order  $s$ ; the asymptotic methods needed to obtain this are a variant of those used above although terms neglected in Eqs (48,61) become important in this region. A schematic of the evolution of a large avalanche is shown in Fig 5. Note that, on average, an avalanche which is going to be large starts with  $m_t$  growing linearly in time, *independent of how big it will become*; this is very different from the behavior of typical avalanches even near to criticality which are small. Nevertheless, typical large avalanches will have large fluctuations of  $m_t$  away from  $\langle m_t | s \rangle$ ; these can be studied by computing, e.g.  $\langle m_t^2 | s \rangle$  from which it can be concluded that a typical  $m_t$  for a large  $s$  avalanche is the same order as  $\langle m_t | s \rangle$  except for  $t \gg \frac{1}{\sqrt{s}}$ . The probability that a large avalanche stops before time  $t$  can be computed from  $\text{Prob}(m_t = 0 | s)$  which is found from  $\Gamma_\infty (\mu_t \rightarrow +i\infty, \mu_\tau = \mu \text{ for } \tau \neq t)$ .

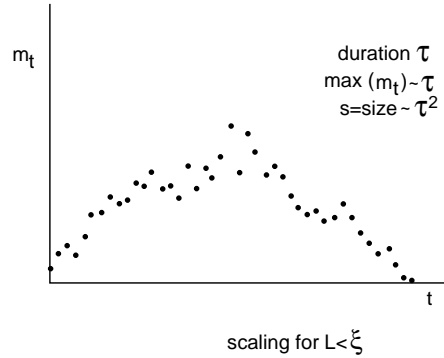


Figure 5: Typical avalanche in a mean field model showing the increase in size of the avalanche,  $m_t$ , at each time step. Note that the fluctuations in  $m_t$  are larger when  $m_t$  is larger.

So far, we have not attempted to relate the local susceptibility to jumps,  $\rho$ , to the original mean field model of the previous section. In general,  $\rho$  will

depend on the past history. But on a generic approach to  $F_c$  from below (e.g. after “training” the system by a slow increase to  $F_c$  from  $F = -F_c$ ),  $\rho$  will approach unity at  $F_c$  and the cutoff  $\tilde{s} \sim \frac{1}{(1-\rho)^2}$  in the jump size distribution will diverge. Right at  $F_c$  there will be a power law distribution of avalanches sizes; this is analogous to the power law distribution of clusters that occur at the critical point for conventional percolation [40].

One might also hope to make connections to power law *spatial* structures at percolation [40] as well as to spatial correlations at conventional equilibrium critical points. But to do this we will certainly have to move away from the infinite-range mean field model. This we do in the next section.

## V. Toy model: spatial structure of avalanches.

The simple mean field model of avalanches discussed in the previous section can be extended in a relatively straightforward way to include spatial and temporal structure like that which arises for general non-negative stress transfer functions  $J(r, t)$ , i.e. monotonic models. Spatial coordinates for  $n(\vec{r}, t)$  are now needed and corresponding generating function variables  $\mu(\vec{r}, t)$ .

In the mean field model, the probability that a segment  $u(\vec{r})$  jumps in a small time interval is proportional to the increase in pulling force  $\phi(\vec{r})$  on it in that interval times a local jump susceptibility  $\rho$ . If we assume the same is true here, then we can generalize the recursion relation equation Eq (42) to include general  $J(\vec{r}, t)$ :

$$\lambda(\vec{r}, t) = \mu(\vec{r}, t) - i\rho \int d\vec{r}' \int_t^\infty dt' J(\vec{r}' - \vec{r}, t' - t) \{ \exp[i\Upsilon \lambda(\vec{r}', t')] - 1 \}. \quad (65)$$

for the case with all jump displacements  $\Upsilon$  equal. Many quantities of interest are computable by similar techniques to those in the previous section, often in terms of the spatio-temporal Fourier transform of  $J(\vec{r}, t)$ ,  $J(\vec{q}, \omega)$ .

The mean number of jumps at  $\vec{r}$  at a time  $t$  after an avalanche is triggered at  $\vec{r} = 0$  at time  $t = 0$  is

$$\langle m(\vec{r}, t) \rangle = \int_{\vec{q}} \int_{\omega} e^{-i\omega t} e^{i\vec{q} \cdot \vec{r}} \frac{1}{1 - \rho \Upsilon J(\vec{q}, \omega)}. \quad (66)$$

The critical point is thus still given by

$$(\rho \Upsilon \tilde{J})_{crit} = 1 \quad (67)$$

with

$$\tilde{J} = J(q = 0, \omega = 0) \quad (68)$$

and the mean total size is

$$\langle s \rangle = \frac{\Upsilon}{1 - \rho \Upsilon \tilde{J}} \quad (69)$$

as before. We will henceforth work in units with  $\Upsilon = \tilde{J} = 1$ .

A more interesting quantity is again the conditional mean:

$$\langle n(\vec{r}, t) | s \rangle = \frac{1}{\text{Prob}(s)} \int_{\mu} \int_{\vec{q}} \int_{\omega} \frac{e^{-i\mu s} e^{i\lambda^*(\mu)} e^{i\vec{q} \cdot \vec{r}} e^{-i\omega t}}{1 - \rho \Upsilon J(q, \omega) e^{i\lambda^*(\mu)}} \quad (70)$$

with  $\lambda^*(\mu)$  the fixed point solution to the mean field recursion relation Eq (42) or, equivalently, Eq (65) with  $\lambda$  and  $\mu$  independent of  $\vec{r}$  and  $t$ . By changing variables one can show that (as in the previous section) conditional statistics like Eq (70) are independent of  $\rho$ .

The important physical quantity is

$$K(\vec{q}, w) \equiv 1 - J(\vec{q}, w) \quad (71)$$

which embodies the information on the space and time dependent elasticity. Changing variables to  $\mu \rightarrow \mu + \text{constant}$  and noting that for large  $s$ , small  $\mu$  will dominate as before, we obtain

$$\begin{aligned} \langle n(\vec{q}, \omega) | s \rangle &\approx \int_{\mu} \sqrt{2\pi s^3} e^{-is\mu} \frac{1}{-i\sqrt{2i\mu} + K(\vec{q}, \omega)} \\ &= \int d\lambda e^{-\frac{1}{2}s\lambda^2} \sqrt{\frac{s^3}{2\pi}} \left[ \frac{\lambda^2}{\lambda^2 + K^2(\vec{q}, \omega)} \right] \end{aligned} \quad (72)$$

For an interface with dissipative dynamics and local elasticity, in the absence of pinning or driving forces we have, after rescaling lengths and times, simply

$$\frac{\partial u}{\partial t} = \nabla^2 u \quad (73)$$

so that

$$K(\vec{q}, \omega) = -i\omega + q^2. \quad (74)$$

But to understand the general behavior, and to apply the results to other physical systems, we would like to include the possibility of long range elasticity, i.e.,

$$\int dt J(\vec{r}, t) \sim \frac{1}{r^{d+\tilde{\alpha}}} \quad (75)$$

in  $d$ -dimensions corresponding to the static

$$\begin{aligned} K_s(\vec{q}) &\sim |q|^{\tilde{\alpha}} \equiv K(\vec{q}, \omega = 0) \quad \text{if } \tilde{\alpha} < 2 \\ \text{or } K_s(\vec{q}) &\sim q^2 \quad \text{if } \tilde{\alpha} > 2. \end{aligned} \quad (76)$$

We thus consider the general case of  $K_s(\vec{q}) \sim |q|^\alpha$  with  $\alpha \leq 2$  with

$$\alpha \equiv \min(\tilde{\alpha}, 2). \quad (77)$$

The total displacement a distance  $r$  from the avalanche starting point, during an avalanche of large size  $s$ , is obtained from Eq (72) with  $\omega = 0$ . We must thus evaluate  $\int_{\vec{q}} e^{i\vec{q} \cdot \vec{r}}$  of the last expression in Eq (72). For  $r = 0$ , all  $q$  can contribute but  $\lambda$  is small so that we can ignore the  $\lambda^2$  in the denominator, yielding

$$\langle \Delta u(r=0) | s \rangle \equiv \Upsilon < \int dt n(r=0, t) | s \rangle \sim \int_{\vec{q}} \frac{1}{[K_s(q)]^2} \quad (78)$$

which is of *order one independent of  $s$*  if

$$d > d_c(\alpha) = 2\alpha. \quad (79)$$

We thus see the appearance of a special *critical dimension* above which no segment will jump more than a few times even in an arbitrarily large avalanche. Indeed, we will see that above the critical dimension driven interfaces will have only bounded small scale roughness.

For  $d < d_c$ , the integral in Eq (78) is infinite so that small  $q$  (i.e. small  $K$ ) dominates and more care is needed. The cutoff of  $\int_q$  of Eq (72) when  $K \sim \lambda$  yields, with a typical  $\lambda \sim \frac{1}{\sqrt{s}}$  and hence  $q \sim s^{-\frac{1}{2\alpha}}$

$$\langle \Delta u(r=0) | s \rangle \sim s^{1-\frac{d}{2\alpha}}. \quad (80)$$

Note the appearance of a non-trivial exponent relating  $\Delta u$  and  $s$ . It depends, as is usually the case for critical phenomena, on the spatial dimension. As



mentioned in the Introduction, Eq (80) is just the kind of scaling law we expect near critical points. Equation (80) relates characteristic scales of displacement to the characteristic scales of avalanche size.

We can also say something about the spatial extent and shape of large avalanches, by computing  $\langle \Delta u(r) | s \rangle$ . For  $d > d_c(\alpha)$ , the integral in Eq (72) will be cutoff for  $q > r$  by the  $e^{iq \cdot \vec{r}}$  oscillations and hence dominated by  $q \sim \frac{1}{r}$  yielding

$$\langle \Delta u(r) | s \rangle \sim \frac{1}{r^{d-2\alpha}} \quad (81)$$

for  $1 \ll r \ll s^{\frac{1}{2\alpha}}$  where the upper cutoff arises when  $K(q \sim \frac{1}{r}) \sim \lambda \sim \frac{1}{\sqrt{s}}$ .

For  $d < d_c$ , on the other hand, as long as  $r \ll s^{\frac{1}{2\alpha}}$ ,  $\int_{\vec{q}} \frac{e^{iq \cdot \vec{r}}}{\lambda^2 + K_s^2}$  for typical  $\lambda$  will be dominated by  $q \sim s^{-\frac{1}{2\alpha}}$  and

$$\langle \Delta u(r) | s \rangle \sim s^{1-\frac{d}{2\sigma}} \quad \text{for } r \ll s^{\frac{1}{2\sigma}}; \quad (82)$$

i.e. the magnitude of typical displacements is approximately independent of  $r$  in this range. In all dimensions,  $\Delta u(r)$  will fall off rapidly for larger  $r$ . The length

$$L \sim s^{\frac{1}{2\alpha}} \quad (83)$$

is thus some measure of the *diameter* of an avalanche.

Let us now try to interpret these results [Note that the skeptic could compute e.g.,  $\langle [\Delta u(r)]^2 | s \rangle$  etc. to provide further support for the picture below]. For  $d > d_c$ , the fact that  $\langle \Delta u(r) \rangle$  is much less than unity for  $r \gg 1$  strongly suggests that *most* segments will *not* jump even if they are within  $r \ll L$  of the avalanche center, rather only a fraction  $\sim 1/r^{d-2\alpha}$  of them will jump, and these typically only once or a few times. The number of sites that have jumped at all within a distance  $R < L$  of the origin is of order  $R^{2\alpha} \ll R^d$  so that the avalanche is *fractal*. The total number of sites that jump, its “area”  $A$  is thus, by taking  $R \sim L$ ,

$$A \sim L^{d_f} \sim s \ll L^d \quad (84)$$

with the fractal dimension

$$d_f = 2\alpha \quad \text{for } d > d_c. \quad (85)$$

In lower dimensions, the picture is quite different. The approximate independence of  $\langle \Delta u(r) | s \rangle$  of  $r$  for  $r \ll L$  suggests that each site in this

region jumps a comparable number of times  $\sim s^{1-d/(2\alpha)}$  (with fluctuations around this of the same order) and hence the avalanche is *not* fractal but has area

$$A \sim L^d \sim s^{\frac{d}{2\sigma}} \quad (86)$$

while the typical displacement is

$$\Delta u(r) \sim L^\zeta \quad (87)$$

for  $r \leq L$  with

$$\zeta = 2\alpha - d. \quad (88)$$

(for  $d > d_c$ ,  $\zeta = 0$ ).

The distribution of  $s$  at the critical point that occurs at  $\rho\tilde{J}\Upsilon = 1$ , is the same as in the mean field model. This implies that

$$\text{Prob (diameter} > L) \sim \frac{1}{L^\kappa} \quad (89)$$

with

$$\kappa = \alpha. \quad (90)$$

The duration of an avalanche with dissipative dynamics—corresponding to

$$K(q, \omega) \approx -i\omega + |q|^\sigma \quad (91)$$

—is given simply by scaling, i.e.,

$$\tau \sim L^z \sim s^{\frac{1}{2}} \quad (92)$$

with the *dynamical critical exponent*

$$z = \alpha. \quad (93)$$

Note that the relation  $\tau \sim \sqrt{s}$  is (not surprisingly) the same as in the infinite-range mean-field model.

We have found that in our toy model, many of the properties of large avalanches near to the critical point (actually *any* large avalanche although they are rare away from criticality), obey scaling laws which relate various characteristic physical properties to each other by power law relationships. For example, for  $d < d_c$ , an avalanche of diameter  $L$  has typical size  $s \sim L^{2\alpha/d}$ ,

displacement  $\Delta u \sim L^\zeta$  and duration  $L^z$ . This type of scaling behavior is one of the key aspects of critical phenomena in both equilibrium and non-equilibrium systems. But there is more: if we scale all lengths by a *correlation length*

$$\xi \sim \epsilon^{-1/\alpha} \quad (94)$$

which is the diameter above which avalanches become exponentially rare, and correspondingly displacements by  $\xi^\zeta$ , durations by  $\xi^z$ , etc., then *functions* such as those that occur in the distribution of avalanche sizes Eq (51), or the average growth of the displacements during an avalanche,  $\langle \frac{\partial u(\vec{r}, t)}{\partial t} | s \rangle$  will be *universal functions of scaled variables* such as  $L/\xi$ . For example, from Eq (72) we obtain, for  $K(\vec{q}, \omega) = -\eta i \omega + D \eta |q|^\alpha$  and  $d < d_c = 2\alpha$ ,

$$\langle \frac{\partial u(\vec{r}, t)}{\partial t} | s \rangle \approx \frac{C_u}{C_t} \xi^{\zeta-z} Y \left( \frac{\vec{r}}{\xi}, \frac{t}{C_t \xi^z}, \frac{s}{C_u \xi^{d+\zeta}} \right) \quad (95)$$

with  $s = \int d\vec{r} \Delta u(\vec{r})$  the total size,  $C_u$  and  $C_t$  *non-universal* (dimensionfull) coefficients which set the scales of the displacements and times; these depend on the random pinning,  $\eta$ ,  $D$ ; etc. The *universal scaling function* is

$$Y(\vec{R}, T, m) = \int_{\vec{Q}} \int_{\Omega} \int d\Lambda e^{i\vec{Q} \cdot \vec{R} - i\Omega T} e^{-\frac{1}{2} m \Lambda^2} \sqrt{\frac{m^3}{2\pi}} \left[ \frac{\Lambda^2}{\Lambda^2 + (-i\Omega + |Q|^\alpha)^2} \right] \quad (96)$$

which depends *only* on the dimension, the range of interactions, and the type of dynamics (i.e. dissipative), as is manifested in the low frequency form of the stress transfer function  $K(\vec{q}, \omega)$ . As we shall see in the next section, a similar scaling structure is expected to exist in more realistic models.

Let us now try applying the toy model results to the interface problem with  $d = 2$  and short range elasticity, so that  $\alpha = 2$ . This dimension is less than

$$d_c^{short-range} = d_c(\alpha = 2) = 4, \quad (97)$$

so we have  $\zeta = 2$ , i.e.  $\Delta u(L) \gg L$ , for large avalanches. But this is clearly unphysical: our original model for the interface assumed that it was close to flat so that, at least on large scales, we need small angles of the interface i.e.  $\nabla u \ll 1$ . Thus the result Eq (87) violates the assumptions of our original model in this case.

What has gone wrong? Is the original model bad or have we made some grievous errors in trying to analyze it? The answer is the latter and understanding why gives some clues as to how to do better.

In the infinite range mean field model, the odds of any given segment jumping more than once are very low as long as  $s \ll \sqrt{N}$ , since the odds of a specific segment jumping at all is small and each jump is almost independent by (justifiable) assumption. But in the finite range models, we assumed that this independence was still true, i.e. that the probability of a segment  $u(\vec{r})$  jumping in a short time interval depends only on the *increase* in pulling force,  $\Delta\phi(\vec{r})$ , on it during that interval. But this is problematic: if a segment has just jumped, it is much less likely to do so again until its neighbors have caught up. The needed increase in  $\phi(\vec{r})$  for a subsequent jump will typically be of order one. [Actually this is true even in our toy model, but the cumulative effect of many jumps causes the problem: the needed  $\Delta\phi(\vec{r})$  to cause a large  $\Delta u(\vec{r})$  that consists of many jumps should be  $\Delta\phi(\vec{r}) \approx \tilde{J}\Delta u(r) \pm O(1)$  while in the toy model it is, for  $\rho = 1$  where large avalanches can occur,  $\Delta\phi(\vec{r}) \approx \tilde{J}\Delta u(r) \pm \tilde{J}\sqrt{\Delta u(r)}$ . This difference is responsible for major errors when avalanches involve large  $\Delta u(r)$ 's but *not* for  $d > d_c(\alpha)$  where  $\Delta u(r)$ 's remain of order one.]

Our task, then, is to somehow take into account properly the anticorrelations between local susceptibilities to successive jumps. This will certainly involve ensuring that the statistical properties of  $\{f_p[\vec{r}, u(\vec{r})]\}$  when all  $u(\vec{r})$  are increased by any fixed amount are preserved; i.e. the *statistical translational invariance* of the system which is lacking in our toy avalanche model.

Remarkably, in spite of its problems the toy model *correctly* gives the statistics and properties of avalanches for large  $s$  and small  $\epsilon$  in dimensions greater than  $d_c(\alpha)$ . The basic reason for this is the observation mentioned above that each segment is unlikely to jump many times during even very large avalanches; a real understanding, however, relies on the renormalization group treatment discussed briefly in the next section.

## VI. Interfaces and Scaling Laws

Motivated by the partial success of the toy model and general scaling concepts from more conventional critical phenomena, we will now approach the interface problem by making a *scaling Ansatz*. Specifically, we conjecture that large avalanches near the critical point have properties which scale with their diameter,  $L$ , (or size  $s$ ) as powers of  $L$  [28][2]. In the toy model we found that the critical exponents which characterized these scaling laws,  $\zeta$ ,  $d_f$ ,  $\kappa$  and  $z$

depend on the dimension of the elastic manifold, the power law decay of the interactions if they are long range, and on the type of dynamics, but *not on other details of the system*. This is the fundamental property of “*universality*”. In contrast, the critical force and coefficients in the scaling functions such as Eq (95), will generally depend on details and hence are non-universal. We might thus hope that in dimensions  $d < d_c(\alpha)$  for which the toy model fails, the exponents will still be universal functions of  $d$  and  $\alpha$ .

In addition to the four exponents already introduced, there should also be an exponent which characterizes the *correlation length*: this is the diameter above which avalanches become unlikely (like  $\xi \sim s_{max}^{\frac{1}{2\alpha}} \sim \epsilon^{-1/\alpha}$  in the toy model) [27]. As  $F$  increases towards  $F_c$  with a generic past history, we conjecture that

$$\xi \sim \frac{1}{(F_c - F)^\nu}. \quad (98)$$

If in the mean field model the local jump susceptibility  $\rho$  is smooth at  $F_c$  [9] so that  $\epsilon \sim F_c - F$ , then  $\nu_{toy-model} = \frac{1}{\alpha}$ . This turns out to be the case for the fuller mean field model defined in section III.

It appears that we have five separate exponents and we would like to understand whether there are some relation among them. Fortunately, this will turn out to be the case. First, however, we can eliminate one exponent.

If, as we expect for  $d < d_c$ ,  $\zeta > 0$  so that some interface segments advance large distances in big avalanches, then the elasticity will certainly make neighboring regions advance as well so that it seems implausible that avalanches would be fractal; thus we expect

$$d_f = d \quad (99)$$

for  $d < d_c$ .

The other relations between exponents are much more subtle. The simplest assumption—and one that is borne out—is that there is one basic length scale  $\xi$  within the interface and a basic scale

$$\Delta u \sim \xi^\zeta \quad (100)$$

in the direction of motion. [Note that we have been sloppy and not put the needed non-universal coefficients, as appeared in Eq (95) into Eq (100).] Thus, for example, if we started with a flat interface and gradually increased

$F$ , when

$$\epsilon \equiv F_c - F \quad (101)$$

is small, the interface would be rough on scales less than  $\xi$ , with

$$\langle [u(\vec{r}) - u(\vec{r}')]^2 \rangle \sim |\vec{r} - \vec{r}'|^{2\zeta} \quad (102)$$

for  $|\vec{r} - \vec{r}'| \ll \xi$ , and be flat on longer scales with

$$\langle [u(\vec{r}) - u(\vec{r}')]^2 \rangle \sim \xi^{2\zeta} \quad (103)$$

for  $|\vec{r} - \vec{r}'| \gg \xi$  as shown in Fig. 6. Similarly, we conjecture that for  $\epsilon$  small, and  $s$  large [2][38]

$$Prob(s) \sim \frac{1}{s^{B+1}} H(s/\xi^{d_f+\zeta}) \quad (104)$$

with  $H(x \rightarrow 0) \rightarrow 1$  and  $H(x \rightarrow \infty) \rightarrow 0$ —i.e., a similar form to that found in the toy model. Scaling implies that the exponent for the distribution of avalanche probability as a function of *diameter* in Eq (89) obeys

$$\kappa = B(d_f + \zeta) \quad (105)$$

We can now compute the “polarizability” of the system

$$\chi \equiv \frac{d \langle u(\vec{r}) \rangle}{dF \uparrow} \quad (106)$$

where the arrow denotes that  $F$  is increasing. This will be given by the sum over avalanches which are triggered with probability  $\rho dF$  per segment of the interface yielding

$$\chi \sim \rho \int \frac{ds}{s} \frac{s}{s^B} H(s/\xi^{d_f+\zeta}). \quad (107)$$

With  $B < 1$ , this is dominated by large  $s$  so that

$$\chi \sim \xi^{(1-B)(d_f+\zeta)} \sim \epsilon^{-(1-B)(d_f+\zeta)\nu}. \quad (108)$$

But from the earlier results about the interface roughness, Eq (103), we also have

$$\chi \sim \frac{d}{dF} \xi^\zeta \sim \epsilon^{-(1+\zeta)\nu}. \quad (109)$$

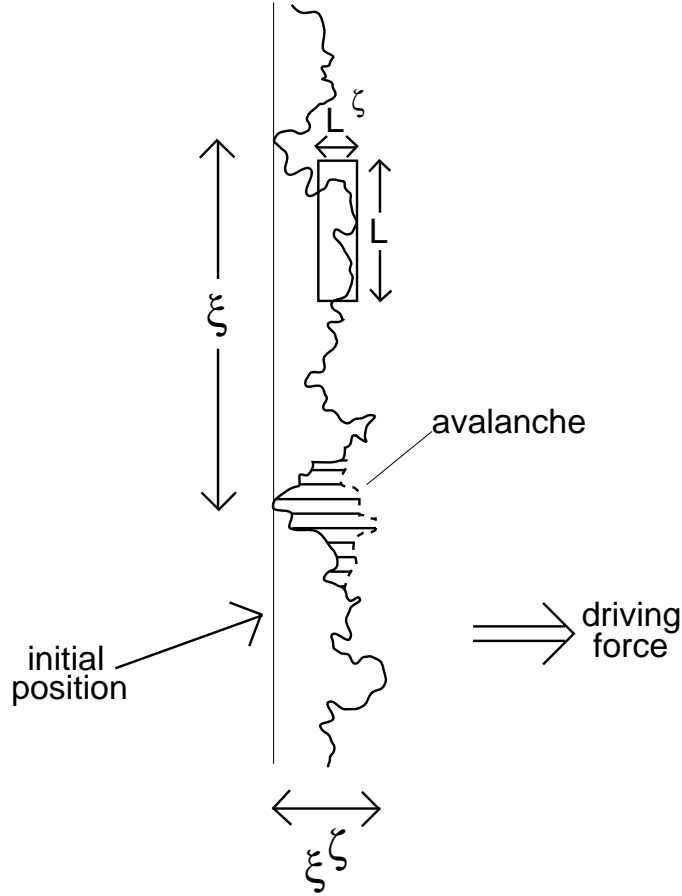


Figure 6: Schematic of a one-dimensional interface with  $F$  somewhat below the critical force. After starting from a flat initial configuration, the typical displacements of the interface are of order  $\xi^\zeta$  with  $\xi$  the correlation length. On smaller length scales, the statistics of relative displacements as a function of separation has a simple scaling behavior as shown. An avalanche that occurs as the force is increased slightly is also shown.

We thus have

$$B = \frac{d_f - \frac{1}{\nu}}{d_f + \zeta} \quad (110)$$

and hence

$$\kappa = d_f - \frac{1}{\nu}. \quad (111)$$

[2] Note that these relations work in the toy model for  $d > d_c(\alpha)$  but *not* for  $d < d_c(\sigma)$  due to the problems discussed earlier.

Another relation can be derived by considering the forces one avalanche exerts on another section of the interface. When an avalanche that moves a region of diameter  $L \sim \xi$  occurs, we expect it to also involve quite a few segments nearby to jump, but not many that are far away. In particular, distances  $R \sim \xi$  away should be borderline. The increase in pulling force from the original part of the avalanche on sections  $\sim R$  away will be

$$\Delta\varphi \sim \xi^{d+\zeta}/R^{d+\alpha} \quad (112)$$

(for short range elasticity,  $\alpha = 2$ , the argument is more subtle). For  $R \sim \xi$ , this  $\Delta\phi$  should be comparable to the deviation  $\epsilon$  from criticality or else we must not have properly identified the crossover distance. Thus we should have

$$\Delta\varphi(R \sim \xi) \sim \frac{1}{\xi^{\alpha-\zeta}} \sim \epsilon \sim \xi^{-\frac{1}{\nu}} \quad (113)$$

yielding the scaling law

$$\frac{1}{\nu} = \alpha - \zeta. \quad (114)$$

A further relation can be derived by considering the variations in the “local critical forces”  $F_{cl}(\vec{r}, L)$  needed to make a region of diameter  $L$  advance by of order  $L^\zeta$ . We define

$$\epsilon_l(\vec{r}, L) \equiv F_{cl}(\vec{r}, L) - F \quad (115)$$

to be, loosely, the deviation from “local criticality”. Since the volume of the region through which the section of scale  $L$  will advance is  $V \sim L^{d+\zeta}$ , we expect that the random pinning forces in the region will make

$$\delta\epsilon_l(L) \equiv \sqrt{\text{variance}[\epsilon_l(\vec{r}, L)]} \geq \frac{1}{L^{(d+\zeta)/2}} \quad (116)$$



i.e. the region “does not know”  $F_c$  to better than this accuracy [10]. If at scale  $L \sim \xi$ ,  $\delta\epsilon_l(L = \xi)$  were much larger than  $\epsilon$ , then we would expect many regions of size  $\xi$  to be unstable so large avalanches that occurred in the past should have been even larger. Thus we should have

$$\delta\epsilon_l(\xi) \leq \epsilon \quad (117)$$

yielding

$$\frac{1}{\nu} \leq \frac{d + \zeta}{2} \quad (118)$$

from Eq (116). This can be combined with Eq (114) to yield

$$\zeta \geq \frac{2\alpha - d}{3}. \quad (119)$$

An upper bound of

$$\zeta \leq 2\alpha - d \quad (120)$$

follows from the observation that the toy model should overestimate the jumps of a typical segment in a large avalanche. For  $d > d_c$ , we expect  $\zeta = 0$ ; i.e. interfaces which are flat on large scales.

So far, we have not discussed the dynamics. One of the (helpful!) features of monotonic models, is that at the end of an avalanche, how much each segment has moved,  $\Delta u(\vec{r})$ , is *independent of the dynamics* although how long the avalanche takes, in what order jumps occur, etc. *will* depend on the dynamics [26][9]. Indeed, even the exponent  $z$  can depend on the stress transfer  $J(\vec{r}, t)$ . In particular for long range interactions whose effect is only felt after a time proportional to  $r$ —i.e. finite velocity of information propagation—one must clearly have  $z \leq 1$  (this can already be seen in the toy model if  $\alpha < 1$ ) [8]. In general, however, we cannot say much about  $z$  without much more work.

Nevertheless, using our scaling Ansatz, we can relate the dynamical behavior in the moving phase for  $F$  just above  $F_c$  to that for  $F < F_c$  [28][2][4]. In particular, we conjecture that the jerkiness of the motion occurs on length scales up to  $\xi \sim \frac{1}{(F - F_c)^\nu}$  and times up to

$$\tau_\xi \sim \xi^z \quad (121)$$

while the motion is smoother on longer scales. This jerky motion will look like the dynamics within avalanches. If we consider, crudely, the motion to

be made up of avalanches of scale  $\xi$  occurring at intervals of order  $\tau_\xi$  within each region of diameter  $\xi$ , then the velocity is simply

$$\bar{v} \sim \frac{\xi^\zeta}{\tau_\xi} \sim (F - F_c)^\beta \quad (122)$$

with

$$\beta = (z - \zeta)\nu. \quad (123)$$

Note again, that with the exponents of the toy model for  $d > d_c$ :  $z = \alpha$ ,  $\nu = \frac{1}{\alpha}$ ,  $\zeta = 0$  and  $\beta = 1$ , the scaling law Eq (123) is obeyed.

In the moving phase, the response of  $\langle u(\vec{r}, t) - \bar{v}t \rangle$  to a small additional *static* force  $\delta F_q e^{i\vec{q} \cdot \vec{r}}$ ,

$$\chi(\vec{q}) = \frac{\delta \langle u(\vec{q}, \omega = 0) \rangle}{\delta F_q}, \quad (124)$$

can be obtained exactly! [Note that here either sign of  $\delta F_q$  is okay if it is sufficiently small.] If the variable change

$$u(\vec{r}, t) = \tilde{u}(\vec{r}, t) + \int_{\vec{q}} e^{i\vec{q} \cdot \vec{r}} \frac{\delta F_q}{\tilde{J} - J(\vec{q}, \omega = 0)} \quad (125)$$

which corresponds to transforming away the response in the absence of pinning, is made, then the *statistical properties* of the random pinning forces

$$\tilde{f}_p[\vec{r}, \tilde{u}(\vec{r}, t)] \equiv f_p[\vec{r}, u(\vec{r}, t)] \quad (126)$$

as a function of  $\tilde{u}$  and  $\vec{r}$  are *identical* to those of the original  $f_p$ . This is a consequence of the underlying statistical rotational invariance of the system [45]. We thus find that

$$\langle \tilde{u}(\vec{r}, t) \rangle_{\delta F_q} = \langle u(\vec{r}, t) \rangle_{\delta F_q=0} \quad (127)$$

so that the average response is given exactly by the second term in Eq (126), i.e.

$$\chi(\vec{q}) = \frac{1}{\tilde{J} - J(\vec{q}, \omega = 0)} \sim \frac{1}{|q|^\alpha}. \quad (128)$$

Since  $\chi$  should scale as  $L^\zeta / L^{\frac{1}{\nu}}$ , we again obtain the scaling law Eq (114). Note that since  $\zeta$  is defined at  $F_c$ , the agreement of this result with that below threshold supports the notion that the appropriate characteristic length

scales above and below threshold will diverge at  $F_c$  with the *same* exponent  $\nu$ .

We have reduced the number of critical exponents to two basic ones;  $\zeta$  and  $z$  which relate displacement and time scales to length scales. But, so far, we have neither a means of computing these exponents; nor more importantly, a way of justifying the scaling laws beyond the hand waving arguments given above (or variants of these); nor even a way of understanding the claimed universality of the exponents.

But with the basic scaling picture in mind, we can try and appeal to the framework of the renormalization group which has been so successful in understanding equilibrium—and some non-equilibrium—critical phenomena. There are two substantial difficulties. One is associated with the basic physics: we must find a way of properly dealing with two kinds of scales in the pinned phase near  $F_c$ . First, the jumps of small segments happen on the basic microscopic time scale but their existence and discrete nature is crucial. Large avalanches last for times which scale with their size out to  $\tau_\xi$  which is very large just below  $F_c$  and thus avalanche activity spans a broad range of scales. But, in addition, there is the time *between* avalanches set by the rate at which  $F$  is changed; as long as this is slow enough, it does not really matter except that the important anti-correlations between successive avalanches in the same region will only be felt on this very long time scale.

The other main difficulty is associated with the history dependence in the pinned phase. For example, what should one average over to get sensible quantities? If the stress transfer,  $J(\vec{r}, t)$ , is non-negative, this difficulty can be circumvented if  $F$  is always increasing (or always decreasing): if this is the case, then from any stable initial condition the pulling force on every segment will increase monotonically with time. This feature is important for the physics as well as drastically simplifying the theoretical analysis. Nevertheless, even in such monotonic models, there will be history dependence. But near to  $F_c$ , this should, at worst, only modify non-universal coefficients as long as the critical force is approached monotonically starting from a much lower force. A natural reproducible history results from starting at  $F = -F_c$ .

For monotonic models, a perturbative renormalization group ( $RG$ ) analysis for dimensions near the upper critical dimension has been carried out [28][2][16]. The first result is that for  $d > d_c(\alpha)$ , the decreased local susceptibility to jumping after a segment has jumped is *irrelevant* in the  $RG$  sense, except on the very long time scales during which the whole system

has advanced. In particular, this justifies our claim that, while the critical force and other non-universal properties will not be given correctly, *universal* features of avalanches such as critical exponents and scaling functions [e.g.  $H$  in Eq (104) and  $Y$  in Eq (95)] *will be given exactly* by the toy model for  $d > d_c$ . In the moving phase, some of the effects left out of the toy model will be important but mean field results like  $\beta = 1$  and  $\zeta = 0$  will obtain [41].

For  $d < d_c$  many new results can be obtained from the RG analysis. In addition to the derivation of universality, scaling laws and perturbative computations of exponents that arise from a new *critical fixed point* of the  $RG$ , it is possible, in principle—although not yet carried out—to compute such quantities as the new universal scaling function that replaces  $Y$  in Eq (95), anticorrelations between avalanches in the same region, local velocity correlations in the moving phase, etc.

Here we just quote the results for the exponents [28][2][16]. All the scaling laws derived heuristically above are found to be obeyed. The exponent  $\zeta$  is

$$\zeta \approx \frac{d_c(\alpha) - d}{3} \quad (129)$$

to all orders in powers of  $d_c - d$ ; indeed, this result—which saturates the lower bound Eq (119)—may well be exact. Numerical computations for  $d = \alpha = 1$  yield

$$\zeta \approx 0.34 \pm 0.02 \quad (130)$$

consistent with  $\frac{1}{3}$  [8][31]. The dynamic exponent is found to be

$$z = \alpha - \frac{2[d_c(\alpha) - d]}{9} + O[(d_c - d)^2]. \quad (131)$$

We thus find an interesting effect: the non-linearities of the avalanche process cause disturbances of the interface to propagate more *rapidly* at long scales than for an unpinned interface. The velocity exponent is then, from scaling,

$$\beta = \frac{z - \zeta}{\alpha - \zeta} \approx 1 - \frac{2(2\alpha - d)}{9\alpha} < 1 \quad (132)$$

i.e. a concave *downwards*  $\bar{v}(F)$  curve. Making the somewhat dangerous extrapolation to the *interface* with  $d = \alpha = 2$ , we get predictions of

$$z \approx \frac{14}{9}, \quad \zeta \approx \frac{2}{3}, \quad \text{and} \quad \beta \approx \frac{2}{3}. \quad (133)$$

At this point, except for some experiments on interfaces between two fluids that are being driven through porous media which give somewhat inconclusive results [37], there are not experiments, of which this author is aware, that test these results for interfaces. But as we shall see in the next section, there have been both experiments and numerical tests carried out on other systems.

## VII. Applications and Complications

In the previous section we saw how scaling ideas and intuition that arise from the simple solvable toy model could be used to develop an understanding of the behavior of interfaces near to the critical driving force that makes them move. Renormalization group methods can then be used to carry out concrete calculations and justify many of the conjectures. In particular, the general *structure* and existence of scaling laws and universality follows rather directly from the existence of an *RG* critical fixed point.

One of the advantages of this framework is that it enables us to apply the general structure to other systems—such as (but not limited to) different dimensionalities and ranges of interactions. But in addition we can introduce various physical features left out of the simple models—even our relatively realistic Eq (3)—and ask whether they are *relevant* in the *RG* sense of changing (or destroying) the universal aspects of the critical behavior. In this section we will discuss several of the physical systems mentioned in the Introduction with an eye both to applying the ideas and seeing how they must be modified—or thrown away!—to account for the appropriate extra physics.

### A. Charge density waves

The best and perhaps really the only real test of critical behavior near to a depinning transition of an elastic manifold in a random medium is that of charge density waves (CDW) driven by an electric field [35]. The periodic electron density waves that occur within this class of materials are incommensurate with respect to the underlying crystalline periodicity in one direction so they could move freely in this direction—contributing to the current proportionally to their velocity—except for being pinned by randomly positioned impurities; see Fig 7. These CDWs are thus three dimensional

elastic manifolds with short range interactions (the coulomb interactions are screened) in a three dimensional random medium. Inertial effects are negligible. The primary difference from interfaces is in terms of the displacements  $u(\vec{r})$ : in the frame of the crystal the random pinning forces  $f_p[\vec{r}, u(\vec{r})]$  are *periodic* in

$$u(\vec{r}) \rightarrow u(\vec{r}) + \lambda_{CDW} \quad (134)$$

for all  $\vec{r}$ , where  $\lambda_{CDW}$  is the wavelength of the CDW. Although the resulting behavior near the critical driving force is not much changed for  $d > d_c = 4$ , the extra symmetry associated with this periodicity changes the *universality class* for  $d < d_c$ . In particular, the exponents become [3]

$$\begin{aligned} \zeta &= 0, \\ \nu &= \frac{1}{2}, \quad \text{and} \\ z &= 2 - \frac{4-d}{3} + O(4-d)^2, \end{aligned} \quad (135)$$

yielding scaling behavior above  $F_c$  involving the velocity exponent

$$\beta = z\nu = 1 - \frac{1}{6}(4-d) + O(4-d)^2 \approx \frac{5}{6} \quad (136)$$

in  $d = 3$ . Experiments [32] carried out on CDWs and numerical simulations yield  $\beta \approx 0.75 - 0.9$  over  $2\frac{1}{2}$  decades of  $F - F_c$ —surprisingly good agreement with the theoretical prediction.

But should we really expect that CDWs will exhibit the critical behavior of an ideal elastic medium? In a precise sense, certainly not. *Thermal fluctuations* (or even quantum fluctuations) can cause sections of the CDW to overcome the barriers caused by the pinning and jump to lower energy local minima. For any non-zero electric field, this will cause the CDW to gradually creep forwards thereby contributing to the current. The critical behavior near the fluctuationless  $F_c$  will thus be smeared out by fluctuations which are hence a *relevant* perturbation [4, 46]. This is quite analogous to the role of a magnetic field near to ferromagnetic phase transitions, which also smears out the critical singularities. But as in the magnetic case, if the perturbation is small enough, critical behavior can still be observed over a wide range of scales and  $F - F_c$  with the smearing only occurring very close to  $F_c$ . In general, fluctuation effects appear to be quite substantial in

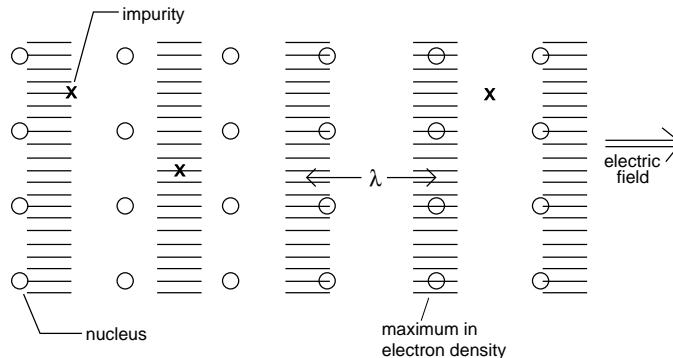


Figure 7: Schematic of a crystal with a charge density wave is incommensurate with respect to the underlying lattice periodicity of the solid. The maxima in the difference between the actual electron charge density and that without the CDW are shown. An electric field pulls on the CDW which could move freely, except for being impeded by pinning forces of the impurities.

CDW systems and the critical behavior is smeared out. But the experiments quoted above [32] were performed by applying an ac driving force in addition to the dc drive; this reduces the effects of thermal fluctuations and appear to yield a wide range over which they do not play much of a role.

Another complication in CDWs—which might also be reduced by an additional ac drive—is *defects* in the CDW lattice, especially dislocations [29]. The pinning is very weak in CDWs implying that the stresses that would cause dislocations to form are unlikely to occur except perhaps on long length scales. In this weak pinning regime, the effects of dislocations are poorly understood. It now appears, however, that dislocations will *not* destroy the existence of the CDW phase in *equilibrium* [11]; this is not directly relevant to the non-equilibrium physics of interest here but may point to progress also on the more relevant issues. Nevertheless, at this point, whether or not defects always destroy the elastic depinning critical behavior that we have studied is an open question.

## B. Superconductors

One system that is quite similar in spirit to a CDW, but for which the strength of the pinning forces can readily be varied, is a *vortex lattice* in a type II superconductor. Vortex lattices are pinned by impurities that impede their motion under the action of a transport current which exerts a force on the vortices [34]. Since the voltage is proportional to the mean vortex velocity,  $\bar{v}(F)$  plots are simply voltage-current curves,  $F_c$  being simply proportional to the *critical current* density.

By making bulk superconducting samples, thin superconducting films or wires, or a normal layer sandwiched between two bulk superconductors, three, two and one dimensional systems can all be studied as well as, in the last case, a two dimensional lattice of roughly parallel vortex lines with no dislocations allowed. In principle, many systems and regimes can thus be investigated, subject to the complication of non-uniform forces on the vortices, dissipative heating effects, and natural tendencies of experimentalists to care more about the magnitude of the critical current density than about what happens when the superconductor fails, i.e. when the critical current is exceeded! Surprisingly, although thermal fluctuation driven transitions in both clean and dirty superconductors have received a lot of attention recently, [34][12] the behavior nearer to critical currents has received far less [23].

If the pinning is very strong, the vortex lattice will be destroyed. What then (when thermal fluctuations can be neglected) will be the qualitative behavior near the critical force? In the case of two dimensional films in a perpendicular magnetic field that produces point-like vortices, the vortex flow just above  $F_c$  will almost certainly be confined to a *sparse* interconnected *network* of irregular *channels* across the system, as sketched in Fig 8. Some preliminary theoretical studies [24] and experiments of the critical behavior that can arise in this regime have been carried out and experiments that "see" the vortices performed [25], but even this simple case is far from understood. For more complicated cases of intermediate strength pinning or when three dimensional effects are important, even less is known.

One thing that is clear, both theoretically [24] and experimentally [23], is that the critical force is history dependent. This and other history dependence—which can be caused by defect motion—is certain to play an important role in the physics. We note that in principle—and soon, if not quite now, in



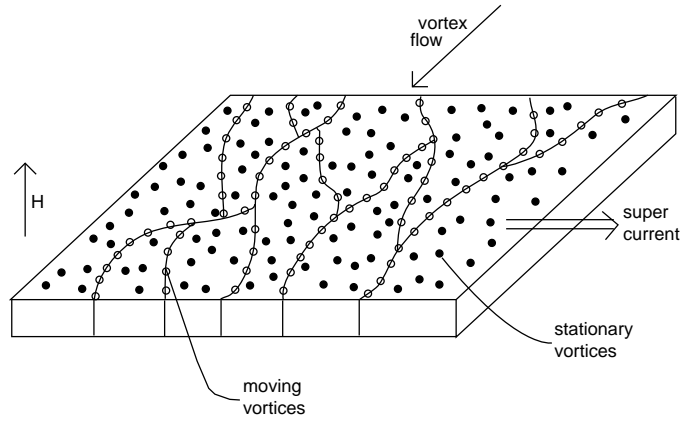


Figure 8: A thin superconducting film in a magnetic field ,  $H$ , perpendicular to the film. A supercurrent provides a driving force for the vortices to move accross the film. Just above the critical current for vortex motion, the vortices in most of the film can remain stationary with the vortex flow confined to a sparse network of vortex channels, as shown. The electric field is proportional to the average vortex flow rate.

practice [25]—measurements of local vortex flow on small scales will be possible in some of the parameter regimes of greatest potential interest. Both macroscopic and microscopic information should be available in these superconducting vortex systems.

Leaving the effects of lattice defects as an intriguing puzzle, we now turn to another type of physical effect that we have so far left out: the role of inertia and other related phenomena.

### C. Cracks

In contrast to CDWs and vortex lattices, interfaces between phases are “topological” and hence have elasticity which is robust for weak pinning, although for strong pinning they can become fractal and a very different “invasion percolation” behavior occurs. Various other elastic systems are also *not* directly susceptible to destruction by defects. In particular, the front of a *planar tensile crack* in a heterogeneous solid has long range  $\frac{1}{r^2}$  elastic forces mediated by the elasticity of the solid which act to keep the crackfront roughly straight; see Fig 9 [6, 30, 15]. But random variations in the local toughness—the energy per unit area needed for crack growth—act to deform the crack front. This system is thus an example of an elastic manifold with  $d = 1$  and  $\alpha = 1$ .

Numerical studies [8][31] with quasistatic (i.e. instantaneous on the time scales of the crack motion) stress transfer which corresponds to  $J(r, t)\alpha\delta(t)/r^2$  and hence is a monotonic system, yields results for  $\zeta$ ,  $z$ ,  $\nu$ , and  $\beta$  in excellent agreement with the  $d = 2 - \epsilon$  expansion results [16]. But the resulting  $z \approx \frac{7}{9}$  is less than one [8, 16]. Therefore, even if the basic propagation of disturbances along the crack front is slow on small scales (so that the quasistatic approximations would seem to be justified), near the critical point disturbances would propagate arbitrarily fast since the characteristic scale of the “velocity” along the crack front would scale as  $\xi/\xi^z$  which diverges as  $\xi \rightarrow \infty$ . This is clearly unphysical and so elastic wave propagation effects *must* change the asymptotic critical behavior. The simplest way to take the time delays associated with wave propagation into account is to use

$$J(r, t) \sim \frac{1}{r^2}\delta(t - r/c) \quad (137)$$

with  $c$  an elastic wave velocity. This is still a monotonic model, so only the dynamic exponent  $z$  will change. Theoretical arguments and numerical

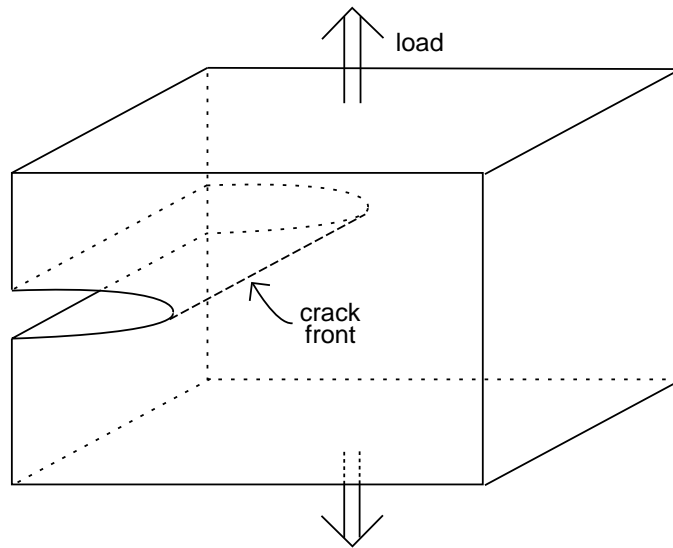


Figure 9: A solid with a crack under tensile loading. If the load is increased, the crack front can progress through the solid. In some circumstances, the crack is confined to a plane; this is the case discussed in the text.

simulations [8] for this case yield  $z = 1$  exactly—so there is no problem with causality. From Eq (123), we obtain  $\beta = 1$ .

But real elastic wave propagation is much more complicated [8][15]. If the crack grows by a segment of the crack front jumping forward only to be stopped by a tougher region, then a point on the crackfront a distance  $r$  away will initially feel no change in stress. Furthermore, when the longitudinal waves with velocity  $c_l$  arrive, the stress that tends to open the crack—analogous to  $\sigma(r, t)$  for the interface model—will actually *decrease* since  $J(r, t \gtrsim r/c_l) < 0$  [7, 8][14]! Only when the Rayleigh waves with slower velocity  $c_R \leq c_t < c_l$  arrive will the opening stress become positive. But when this occurs, there will be a rapid jump to a *large peak* value of the opening stress followed by a gradual fall off to the eventual static stress increase which is

$$J(r, \omega = 0) = \int_0^\infty J(r, t) dt \sim \frac{1}{r^2}. \quad (138)$$

This is highly non-monotonic behavior! Such *stress overshoots* can cause segments of the crack front to jump forward that would *not* have been triggered by the static stress changes. How often this occurs will depend on the heights of the stress peaks relative to the static stress increases—i.e. to the size of the overshoots. If the jumps of segments of the crack are slow and smooth (with duration long compared to the sound travel time across the jumping segment) then the stress overshoots will only occur far from the jumping segment and have small amplitude. Their effects should then be small and the quasistatic behavior should be observable—except, as we shall see, very near  $F_c$ . But *any* stress overshoots will at least occasionally cause *some* extra jumping and we must understand their effect.

Some intuition can be gleaned by considering what would happen if the stress increases *never* decayed to their static value, but stayed at their peak strength. This would correspond, roughly, to increasing the elastic interactions of the crack with itself. As we saw in the mean field model, such enhanced elasticity causes the critical force to decrease because of more effective averaging over the randomness [see Eq (20)]. Thus we would expect avalanches to run away at a force *below* the quasistatic  $F_c$ . A careful analysis of the effects of realistic stress transfer peaks followed by decay towards the static stress shows that the same basic picture obtains [5][8].

Consider a segment which, at the end of the quasistatic approximation to an avalanche, has a final stress on it which is very close to being enough

to make it jump again. Then any overshoot in the stress on this segment that occurred during the actual avalanche will, if the resulting peak stress is above the quasistatic final stress, cause it to undergo an extra jump. If, as is indeed the case, there is a small density of these extra jumps roughly randomly distributed within the avalanche, each of the extra jumps will trigger extra avalanches, for which one again has to consider the effects of the stress overshoots which make more avalanches, etc. One can show that this process will *always* run away for a sufficiently large avalanche—independent of how small the stress overshoots might be [8, 5].

The stress peaks are thus a *relevant* perturbation which will change the critical behavior. Indeed, the runaway of large avalanches implies the *coexistence of moving and stationary states* and strongly suggests that the depinning transition in the presence of stress pulses will be either *first order* with a discontinuous and probably hysteretic  $\bar{v}(F)$  or have a continuous  $\bar{v}(F)$  but with a smaller critical force and different critical behavior [8].

What happens if the stress overshoots are small, say with strength parameterized by  $\Sigma$ ? Then only avalanches with

$$L \geq L_\Sigma \sim \frac{1}{\Sigma^{1/y_\Sigma}} \quad (139)$$

will typically be much affected by the stress peaks. The exponent  $y_\Sigma$  is the RG eigenvalue for the relevant perturbation,  $\Sigma$ ; it has been computed analytically [5, 8] and checked numerically [8] for some types of stress overshoots, but its value is not yet understood analytically for the type of long-tail stress peaks that occur in the crack problem [8, 14].

Experiments on very slowly advancing cracks confined to a plane [17] yield an estimate of the roughness exponent which characterizes the deviations of the crack front from a straight line, of

$$\zeta_{\text{crack front}} \approx 0.55 \pm .05 \quad (140)$$

substantially larger than the quasistatic prediction of  $\frac{1}{3}$ . However the large corrections to scaling predicted by the RG analysis [8][19] may account for this discrepancy; beware of quoted error bars for exponents! It is possible, however, that real elastodynamic effects play a role even for slowly moving planar cracks.

A related challenge is to understand the crack front distortions which manifest themselves in the roughness of the *fracture surface* left behind after a crack front passes: i.e. after the material is broken [18][30][7]. Again,

elastodynamic effects may play a crucial role. In certain situations, cracks can form multiple branches –such as shattering of glass–, or just a few small branches near the crack front [15]. Under what circumstances crack branching effect might affect the onset of crack motion or the large scale shape of fracture surfaces is another open question.

#### D. Faults

So far—except for crack front roughness—we have only discussed systems for which the simple measurements are of macroscopic properties such as  $\overline{v}(F)$ . But there is one natural system in which, even though the length scales are huge, the measurements are of “microscopic” type: specifically, the statistics and other properties of “avalanches”.

A crude model of a geological fault is the motion of two large blocks of crust in contact along a disordered but roughly planar surface—the fault—which move relative to each other; see Fig 10. The motion is driven by forces exerted from far away (e.g. from the viscoelastic region beneath the crust) that are transmitted to the fault by the elasticity of the blocks. Rather than being driven by a constant force, the blocks are driven at a fixed time-averaged velocity that is extremely slow—of order millimeters to centimeters per year—compared to other characteristic velocities—e.g. the speed of sound in the rock [43]. Segments of the two dimensional fault plane interact with each other by long range  $\frac{1}{r^3}$  stress transfer –as can be seen by dimensional analysis– and are pinned by heterogeneities on the two fault surfaces that have to rub past each other [5].

Earthquakes, of course, are just the “avalanches” that occur when some segment of the fault becomes unpinned and jumps forward triggering others [47, 13]. The range of length scales of slipping regions is huge: from meters to hundreds of kilometers, with slips—changes in relative displacement across the fault plane, i.e.  $\Delta u$ —from millimeters to tens of meters.

Most theoretical approaches to modelling faults have involved physics driven by friction laws and inertial effects [20], with intrinsic heterogeneities playing a secondary role if included at all. An alternative approach [5], motivated by the systems we have discussed here, might be to start from the opposite end, a strongly disordered fault with quasistatic stress transfer, and then bring in other features such as elastic wave propagation (which is the manifestation of inertia) and frictional weakening. This has the advantage of

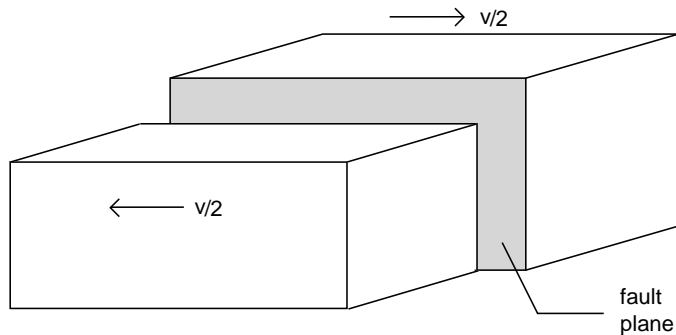


Figure 10: Schematic of two segments of crust which move relative to each other along a fault plane in a sequence of earthquakes. The driving forces are transmitted to the fault by the two halves of the crust moving with relative velocity,  $v$ .

building on an established theoretical framework in which the importance—or lack thereof—of various features can be considered. This is particularly useful as the parameter space in even relatively simple models is very large and thus hard to explore numerically—at least in ways that might convince a skeptic of the interpretations or predictions!

If the forces that one side of the fault exerts on the other are independent of the history and the local slip velocities  $\frac{\partial u(\vec{r}, t)}{\partial t}$  and the stress transfer is quasistatic, i.e.  $J_{qs} \sim \delta(t)/r^3$ , then this system falls into the class of generalized interface models with  $d = 2$  and  $\alpha = 1$ . But for this  $\alpha$ , two is exactly the upper critical dimension so we can use the results of the toy model. The fault system acts as if it were driven just below  $F_c$  (by an amount that goes to zero for large system size) so that we can set  $\epsilon = 0$  [49]. [Note that there should be logarithmic corrections to various quantities, as is usual at critical dimensions, but their effects are small]. The toy model is sufficiently simple, that one can include a realistic way of driving the faults, but for now we consider the simpler idealized infinite system.

Several results can immediately be used [5]: the area of the region of the fault that slips in an earthquake will scale as the square of its diameter,  $L$ , the typical slip in this region will depend only logarithmically on  $L$  (i.e.

$\zeta = 0$ ), and the size, in this context called the *moment*, will scale as

$$M = \int d\vec{r} \Delta u(\vec{r}) \sim L^2. \quad (141)$$

Note that the *moment magnitude* often quoted in newspapers is

$$m = \log_{30} M + \text{constant}, \quad (142)$$

the base 30 being for historical reasons, particularly consistency with the older Richter magnitude scale. The probability of different sized events in the simple model is

$$\text{Prob}(\text{moment} > M) \sim \frac{1}{M^B} \quad (143)$$

with  $B = \frac{1}{2}$ .

How do these predictions compare with observations? The moment of quakes is the best measured quantity, although for medium and larger size events, the duration  $\tau$  can also be measured well. The diameter—or generally the dimensions of the slipped region—and the slip  $\Delta u$  can only be measured directly if the quake involves slip where the fault breaks through the surface of the earth. However, earthquake data are usually interpreted in terms of a *crack picture* in which  $\zeta = 1$  and  $z = 1$  so that

$$M_{\text{crack}} \sim L^3 \sim \tau^3 \quad (144)$$

[43]. This scaling appears to be reasonably well justified observationally for large earthquakes and the  $M \sim \tau^3$  scaling perhaps also for intermediate size events. But for small events—i.e. most of them—only the moment can be measured reasonably reliably. Thus, perhaps, our  $M \sim L^2 \sim \tau^2$  might not be ruled out for small events although it probably is for large ones. Note however, that in quakes of magnitude  $m = 7$  or so and above, the linear size (e.g. the diameter) is comparable to the depth of the crust (and other relevant length scales) so different scaling laws should in any case be expected for large earthquakes with a crossover between the two regimes [42].

The question of earthquake magnitude statistics is a complicated and controversial one. The famous Gutenberg-Richter law [22] states that the distribution of *all* earthquakes approximately satisfies Eq (143) with a  $B \approx \frac{2}{3}$ ,



although it changes somewhat—perhaps for the reasons mentioned above—around magnitude seven. The data cover over twelve orders of magnitude in the moment, equivalent to, assuming the crack scaling Eq (144), four orders of magnitude in length scale. Understanding the Gutenberg-Richter law is a very interesting problem, tied closely to that of understanding the apparent fractal distribution of some geological features such as fault networks [13]. But our subject here is individual faults—at least if they really exist as well defined entities, a question which is also controversial. Observations of some highly disordered faults have been fitted—over a reasonable range—with  $B \sim 0.5 - 0.6$  [21]. This is perhaps encouraging although the apparent rough agreement with our Eq (143) may well be fortuitous. Most faults, however, exhibit quite different behavior: a small regime (if at all) of power law statistics that can be fit by somewhat larger  $B$ 's, then a gap with few events and a narrow peak (which dominates the total slip) at a *characteristic earthquake* size in which the whole fault section slips [21]. This behavior, sketched in Fig 11b, appears to be very different from the power-law scaling behavior we have found in our simple quasistatic heterogeneous model. However, behavior qualitatively similar to Fig 11b—with large characteristic earthquakes—has been found in simulations of models with inertia and frictional weakening but no intrinsic randomness although analytic understanding of these results is rather limited [20].

Can we understand qualitatively how both power-law and characteristic-earthquake types of behavior might arise starting from our simple randomness-dominated picture? Elastodynamic effects, as for the crack front problem discussed earlier, will result in peaks in the dynamic stress transfer that are larger than the static stress transfer. In addition, frictional weakening—the tendency for dynamic frictional forces to be less than static frictional forces—will also be present. Both of these effects will cause extra segments to slip that would not have slipped in quasistatic events. These, as for the crack front, will cause runaway of large earthquakes which will eventually be stopped only by strong “pinning” caused by the boundaries of the fault section, or by the unloading of the shear stress that is driving the fault. If the stress overshoot and frictional weakening effects are small, there should be a wide regime of power law scaling with  $B = \frac{1}{2}$  which can extend out to the largest quakes in the fault section. But if these effects are strong—as one might guess would be the case for a weakly disordered fault that is close to planar—intermediate size events will not occur and the behavior will be

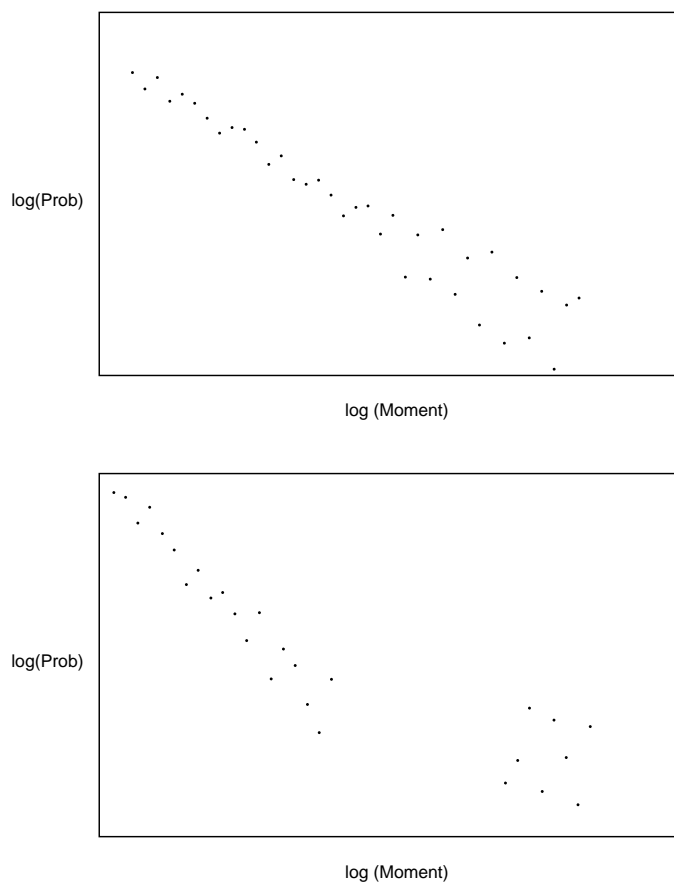


Figure 11: Schematic of two types of earthquake statistics observed on different geological faults; see [20] . The probability of quakes with a given moment is plotted on a log-log scale. a) A fault with power law statistics of events. b) A fault that exhibits “characteristic earthquake” behavior which refers to the peak in the distribution for large events of a characteristic size, with not many intermediate size events occurring.

qualitatively similar to the characteristic- quake behavior observed in many faults [5]. Which behavior obtains would be determined by how the length scale above which events typically runaway compares with the length of the fault section.

Although this basic scenario of fault dynamics that was found in the simple heterogeneous fault model may have nothing to do with what happens in the real earth, analog laboratory systems might be found—or synthesized—in which some of these ideas could be tested.

In these lecture notes, we have outlined a framework for studying the non-equilibrium "critical" behavior that occurs near the onset of macroscopic motion in many driven systems. This enables us to understand the origins, nature, and statistics of avalanche-like events that can occur in these systems, as well as other qualitative and quantitative aspects of the critical behavior. But the examples given in this section have also illustrated a key point of these lectures: to be really useful, a phenomenological framework should be broad enough and robust enough to show the roots of its own failure. With judicious choice of which experimental systems to focus on – and some luck – this should enable enough predictions to be made that theoretical results and underlying assumptions built into models are falsifiable!

## ACKNOWLEDGEMENTS

Whatever understanding the author might have of the problems discussed here is due in large part to interactions over the past fifteen years with students, postdocs and colleagues too numerous to mention. To all of them, I am most grateful. I would also like to thank Jennifer Schwarz for comments on a preliminary version of the manuscript. This work has been supported in part by the National Science Foundation via grants DMR 9106237, DMR 9630064, and Harvard University's MRSEC.

## References

- [1] **NOTE ON REFERENCES** Since the literature in many of the areas discussed here is vast, I have generally tried to include references to papers that elucidate the main points using a framework similar to that of these notes, to review or introductory articles, and to recent papers that contain references to earlier literature, rather than referring directly to all the relevant original papers.
- [2] O. Narayan and D.S. Fisher, Phys. Rev. B **48**, 5949 (1993). The renormalization group analysis is based on that in [3].
- [3] O. Narayan and D.S. Fisher, Phys. Rev. B **46**, 11520 (1992).
- [4] D.S. Fisher, Phys. Rev. B **31**, 1396 (1985).
- [5] D.S. Fisher, K. Dahmen, S. Ramanathan and Y. Ben-Zion, Phys. Rev. Lett. **78**, 4885 (1997).
- [6] S. Ramanathan, D. Ertas and D.S. Fisher, Phys. Rev. Lett. **79**, 873 (1997).
- [7] S. Ramanathan and D.S. Fisher, Phys. Rev. Lett. **79**, 877 (1997).
- [8] S. Ramanathan and D.S. Fisher, in preparation; S. Ramanathan, PhD Thesis, Harvard University, 1997.
- [9] A.A. Middleton and D.S. Fisher, Phys. Rev. B **47**, 3530 (1993).
- [10] J.T. Chayes, L. Chayes, D.S. Fisher and T. Spencer, Phys. Rev. Lett. **57**, 299 (1986); Comm. Math Phys. **120**, 501 (1989) present rigorous results and generalizations of a result of A.B. Harris, J. Phys. C **7**, 1671 (1974) on correlation length exponents in random systems.
- [11] The possible stability to dislocations of an elastic solid in a three dimensional weakly random medium has been discussed by various authors including J. Kierfeld, T. Natterman, and T. Hwa, Phys. Rev. B **55**, 626 (1997); T. Giamarchi and P. LeDoussal, Phys. Rev. B **52**, 1242 (1995); D.S. Fisher, Phys. Rev. Lett. **78**, 1964 (1997); see also [34].

- [12] D.S. Fisher, M.P.A. Fisher and D.A. Huse; Phys. Rev. B **43**, 130 (1991); see D.A. Huse, D.S. Fisher and M.P.A. Fisher, Nature **358**, 553 (1992) for an introduction to the basic issues involved.
- [13] Various authors have studied the development and dynamics of fault networks using models that are somewhat related to those discussed here; see, e.g., K. Chen, P. Bak, S.P. Obukhov, Phys. Rev. A **43**, 625 (1991); P.A. Cowie, C. Vanneste, and D. Sornette, J. Geophys. Res. **98**, 21809 (1993); P. Miltenberger, D. Sornette and C. Vanneste, Phys. Rev. Lett. **71**, 3604 (1993); and references therein.
- [14] J.R. Willis and A.B. Movchan, J. Mech. Phys. Solids **43**, 319 (1995).
- [15] For a general reference on analytical work on fracture dynamics, see L.B. Freund, *Dynamic Fracture Mechanics*, (Cambridge University Press, Cambridge, 1990); and for a more phenomenological treatment, see B. Lawn *Fracture of Brittle Solids*, (Cambridge University Press, Cambridge, 1993).
- [16] E. Ertas and M. Kardar, Phys. Rev. E **49**, R 2532 (1994).
- [17] J. Schmittbuhl and K.J. Måløy, Phys. Rev. Lett. **78**, 3888 (1997).
- [18] E. Bouchaud, J. Phys. C **9**, 4319 (1997) and references therein.
- [19] O. Narayan, private communication.
- [20] See, e.g. J.M. Carlson, J.S. Langer, and B.E. Shaw, Rev. Mod. Phys. **66**, 658 (1994) and references therein.
- [21] S.G. Wesnowsky, [Bull. Seismol. Soc. Am. **84**, 1940 (1994)] has analyzed the statistics of earthquakes on various faults in California.
- [22] B. Gutenberg and K.F. Richter, Ann. Geophys. **9**, 1 (1996).
- [23] See, e.g. M.J. Higgins and S. Bhattacharya, Physica C **257**, 232 (1996).
- [24] J. Watson and D.S. Fisher, Phys. Rev. B **54**, 938 (1996); Phys. Rev. B **55**, 14909 (1997); A.-C. Shi and A.J. Berlinsky, Phys. Rev. Lett. **67**, 1926 (1991).

- [25] T. Matsuda et al, Science **271**, 1393 (1996).
- [26] A.A. Middleton, Phys. Rev. Lett. **68**, 670 (1992).
- [27] O. Narayan and A.A. Middleton, Phys. Rev. B **49**, 244 (1994).
- [28] T. Natterman, S. Stepanow, L.-H. Tang and H. Leschorn, J. Phys. (France) II **2**, 1483 (1992).
- [29] S.N. Coppersmith, Phys. Rev. Lett. **65**, 1044 (1990).
- [30] H. Larralde and R.C. Ball, Europhys Lett. **30**, 287 (1995).
- [31] Other authors have found  $\zeta \approx \frac{1}{2}$ ; see J. Schmittbuhl, S. Roux, J.-P. Vilotte and K.J. Måløy, Phys. Rev. Lett. **74**, 1787 (1995) and P.B. Thomas and M. Paczuski, cond-mat 9602023. It is not clear whether the differences between these results and  $\zeta \approx \frac{1}{3}$  can be attributed to corrections to scaling or to some other source.
- [32] M.Y. Higgins, S. Bhattacharya and A.A. Middleton, Phys. Rev. Lett. **70**, 3784 (1993).
- [33] see P.C. Hohenberg and B.I. Halperin, Rev. Mod. Phys. **49**, 435 (1977) for a review of equilibrium dynamic critical phenomena.
- [34] G. Blatter, M.V. Feigelman, V.B. Geshkenbein, A.I. Larkin and V. Vinokur, Rev. Mod. Phys. **66**, 1125 (1988) and references therein. For a general introduction to vortex dynamics, see M. Tinkham *Introduction to Superconductivity, 2nd Edition* (McGraw-Hill, New York, 1996).
- [35] G. Gruner, Rev. Mod. Phys. **60**, 1075 (1988) and references therein.
- [36] P.G. de Gennes, Rev. Mod. Phys. **57**, 827 (1985).
- [37] J.B. Stokes, D.A. Weitz, J.P. Gollub, A. Dougherty, M.O. Robbins, P.M. Chaikin and H.M. Lindsay, Phys. Rev. Lett. **57**, 1718 (1986).
- [38] The importance of “avalanche” like phenomena in a variety of physical systems has been emphasized by P. Bak, C. Tang and collaborators, see e.g. P. Bak, C. Tang and C. Wiesenfeld, Phys. Rev. Lett. **59**, 381 (1987); P. Bak and K. Chen, Sci. Amer. **264**, 46 (1991), and this and other

- critical-like phenomena dubbed “self-organized criticality”. See also [49, 47].
- [39] The scaling law for distribution of avalanche sizes is the same as that in mean field models of “sandpiles”, (see P. Bak and C. Tang, J. Stat. Phys. **51**, 797 (1988)) as well as that of cluster sizes in the mean field theory of percolation [40].
  - [40] D. Stauffer and A. Aharony, *Introduction to Percolation Theory*, 2nd ed. (Taylor & Francis, London 1991).
  - [41] The velocity exponent,  $\beta$ , in mean field theory is not fully universal. It depends on whether or not the pinning forces are continuously differentiable and, if not, on the nature of the singularities in  $f_p(u)$ . For all but discontinuous forces, this causes long time scales in mean-field theory associated with the acceleration away from configurations that have just become unstable. With short range interactions, these should not play a role due to the jerky nature of  $\varphi(\vec{r}, t)$  caused by jumps. Thus the mean-field models with  $\beta_{MF} = 1$  are the “right” ones about which to attempt an RG analysis. See [48]
  - [42] J.F. Pacheco, C.H. Schulz, and L.R. Sykes, Nature **355**, 71 (1992).
  - [43] For a general reference on earthquake dynamics, see e.g. K. Kanimori and E. Boschi, eds. *Earthquakes: Observation, Theory, and Interpretation* (North Holland, Amsterdam 1983).
  - [44] K. Dahmen and J.P. Sethna, Phys. Rev. B **53**, 14872 (1996).
  - [45] If the system is not rotationally invariant, the depinning critical behavior can be very different; see the discussion in [48].
  - [46] A. A. Middleton, Phys. Rev. B **45**, 9465 (1992).
  - [47] D.S. Fisher *Friction and Forced Flow: Collective Transport in Disordered Media*, in *Nonlinearity in Condensed Matter*, ed. by A. R. Bishop, D.K. Campbell, P.Kumar and S. Trullinger, (Springer-Verlag, New York, 1987).
  - [48] M. Kardar, in this volume.

- [49] Whether critical behavior is considered "self-organized" or not is somewhat a matter of taste: if the systems we are considering are driven at very slow velocity, then they will be very close to critical. In another well known situation, when a fluid is stirred on large scales, turbulence exists on a wide range of length scales extending down to the scale at which viscous dissipation occurs. In both of these and in many other contexts the parameter which is "tuned" to get a wide range of scales is the ratio of some basic "microscopic" scale to the scale at which the system is driven.